NACA RM L57L17a

NACA

RESEARCH MEMORANDUM

EFFECTS OF CANARD SURFACE SIZE ON STABILITY AND CONTROL CHARACTERISTICS OF TWO CANARD AIRPLANE CONFIGURATIONS AT MACH NUMBERS OF 1.41 AND 2.01

By M. Leroy Spearman and Cornelius Driver

Langley Aeronautical Laboratory
Langley Field, Va.

NATIONAL ADVISORY COMMITTEE FOR AERONAUTICS

WASHINGTON

March 16, 1958
Declassified October 28, 1960

NATIONAL ADVISORY COMMITTEE FOR AERONAUTICS

RESEARCH MEMORANDUM

EFFECTS OF CANARD SURFACE SIZE ON STABILITY AND CONTROL CHARACTERISTICS OF TWO CANARD AIRPLANE CONFIGURATIONS AT MACH NUMBERS OF 1.41 AND 2.01

By M. Leroy Spearman and Cornelius Driver

SUMMARY

An investigation has been conducted in the Langley 4- by 4-foot supersonic pressure tunnel to determine the stability and control characteristics of two canard airplane configurations equipped with various sizes of canard control surfaces. Two wings of equal area but differing in plan form were investigated. One wing had a trapezoidal plan form with an unswept 80-percent-chord line, an aspect ratio of 3, and a taper ratio of 0.143; the other wing had a 60° delta plan form with an aspect ratio of 2.31. The trapezoidal canard surfaces investigated had ratios of exposed area to total wing area of 0.051, 0.062, 0.082, and 0.096. The model was equipped with a low-aspect-ratio vertical tail and twin ventral fins.

In general, the experimentally determined variations of control effectiveness C_{m_δ} and longitudinal stability $\partial C_m/\partial C_L$ with canard surface area were in good agreement with estimated variations.

The maximum trimmed lift-drag ratio increased with increasing canard size for a constant center-of-gravity position because of a decrease in stability. For a constant static margin, however, the maximum lift-drag ratio was only slightly less with the smallest canard than with the largest.

The effects of canard size on the sideslip derivatives were relatively small; however, variations in the center-of-gravity position that are effective in altering the longitudinal trim characteristics may be limited by the directional-stability requirements.

INTRODUCTION

In view of the supersonic performance gains that might be realized from the relatively high values of lift-drag ratio obtainable with canard configurations, a research program was initiated at the Langley 4- by 4-foot supersonic pressure tunnel to determine the aerodynamic characteristics of a generalized canard airplane configuration at supersonic speeds. Two configurations differing only in wing plan form were investigated. One wing had a trapezoidal plan form with an unswept 80-percent-chord line, an aspect ratio of 3, and a taper ratio of 0.143. The other wing had a 60° delta plan form with an aspect ratio of 2.31. Each configuration had a trapezoidal canard surface and was equipped with a low-aspect-ratio swept vertical tail and twin ventral fins. The results of an investigation of longitudinal and lateral stability and control are presented in reference 1 for the configurations at Mach numbers of 1.41 and 2.01.

In order to determine the effects of canard surface size on the aerodynamic characteristics of the configurations, the investigation has been extended to include canard surfaces having ratios of exposed area to total wing area of 0.051, 0.062, 0.082, and 0.096, and the results are presented herein.

SYMBOLS

The results are presented as force and moment coefficients with lift, drag, and pitching moment referred to the stability-axis system and rolling moment, yawing moment, and side force referred to the body-axis system (fig. 1). The reference center of moments (center of gravity) was at body station 25 (fig. 2).

C_L lift coefficient, $\frac{F_L}{qS_w}$

$C_{D'}$ drag coefficient, $\frac{F_{D'}}{qS_w}$

C_m pitching-moment coefficient, $\frac{M_{Y_s}}{qS_w\bar{c}_w}$

C_l rolling-moment coefficient, $\frac{M_X}{qS_wb}$

C_n	yawing-moment coefficient, $\frac{M_Z}{qS_w b}$
C_Y	side-force coefficient, $\frac{F_Y}{qS_w}$
F_L	lift force
F_D'	drag force
M_Y	moment about Y-axis
M_X	moment about X-axis
M_Z	moment about Z-axis
F_Y	side force
q	free-stream dynamic pressure
S_w	wing area including fuselage intercept
S_c	exposed area of canard
b	wing span
$\bar{c}_w$	wing mean geometric chord
M	free-stream Mach number
α	angle of attack, deg
β	angle of sideslip, deg
δ_c	angle of canard deflection, deg
Λ	sweep angle, deg
t	section thickness
l_c	length between canard hinge line and center of gravity
x	distance along X-axis

C_{n_β} directional-stability parameter, $\frac{\partial C_n}{\partial \beta}$ per degree

C_{l_β} effective-dihedral parameter, $\frac{\partial C_l}{\partial \beta}$ per degree

C_{Y_β} side-force parameter, $\frac{\partial C_Y}{\partial \beta}$ per degree

$\frac{\partial C_m}{\partial C_L}$ longitudinal-stability parameter

C_{m_δ} rate of change of pitching-moment coefficient with canard deflection for a constant angle of attack, $\frac{\partial C_m}{\partial \delta_c}$ per degree

$\frac{S_c l_c}{S_w \bar{c}_w}$ canard volume coefficient

L/D lift-drag ratio, C_L/C_D

Subscript:

s denotes stability-axis system

MODELS AND APPARATUS

Details of the model components are shown in figures 2 and 3, and the geometric characteristics are presented in table I.

The body of the model was composed of a parabolic nose followed by the frustum of a cone which was faired into a cylinder. The body fineness ratio was 10.57. Coordinates of the body are given in table II. The delta and trapezoidal wings had equal areas. The ratios of exposed canard area to total wing area were 0.051, 0.062, 0.082, and 0.096. All canard surfaces were located with their hinge lines at body station 9.125, with the exception of one arrangement wherein the canard surface $(S_c/S_w = 0.062)$ was located with its hinge line at body station 2.340. The canard in the forward position was identical in plan form to the canard in the normal position but differed in that the section was a flat plate with a thickness of 0.0625 inch, and the deflection angle

was fixed at 0°. All canard surfaces except the one in the forward position were motor driven, and the deflections were set by remote control.

Force and moment measurements were made through the use of a six-component internal strain-gage balance. The model was mounted in the tunnel on a remote-controlled rotary sting.

TESTS, CORRECTIONS, AND ACCURACY

The test conditions are as follows:

	M = 1.41	M = 2.01
Stagnation temperature, °F	100	100
Stagnation pressure, lb/sq ft abs	1,440	1,440
Reynolds number based on $\bar{c}_w$ of delta wing	3.24×10^6	2.68×10^6
Reynolds number based on $\bar{c}_w$ of trapezoidal wing	2.54×10^6	2.10×10^6

The stagnation dewpoint was maintained sufficiently low (-25° F or less) so that no condensation effects were encountered in the test section.

The angle of incidence was corrected for the deflection of the balance and sting under load. The base pressure was measured, and the chord force was adjusted to a base pressure equal to free-stream static pressure.

The estimated maximum variations in the individual measured quantities are as follows:

C_L	±0.0003
$C_{D'}$	±0.001
C_m	±0.0004
C_l	±0.0004
C_n	±0.0001
C_Y	±0.0015
α, deg	±0.2
β, deg	±0.2
δ_c, deg	±0.1
M	±0.01

RESULTS AND DISCUSSION

Longitudinal Characteristics

The effects of canard size on the aerodynamic characteristics in pitch for the delta-wing and trapezoidal-wing configurations are shown in figures 4 and 5, respectively. The variations of pitching moment with lift for the configurations with the canard off are generally linear and indicate no unusual characteristics. With the addition of the canard surface and with increasing canard size, of course, the longitudinal stability decreases and a gradual tendency toward reduced stability at high lifts is apparent. This tendency toward reduced stability could result in pitch-up for lower static margins.

The addition of the canard surface generally results in an increase in lift-curve slope, an increase in minimum drag, and a decrease in the drag due to lift. These characteristics are generally accentuated as the canard surface size is increased.

The longitudinal-control data for the various configurations are presented in figures 6 to 9. Deflection of the canard controls provides essentially constant increments of pitching moment throughout the lift range that increase as the canard size is increased. Contrary to the usual loss of lift associated with the deflection of rearward controls, deflection of the canard control generally has little effect on the lift at a constant value of α and in some cases even provides a measurable increase in lift. (See fig. 9(c), for example.)

The effect of the longitudinal position of the canard was determined for one configuration with $\delta_c = 0^\circ$ (delta wing, $S_c/S_w = 0.062$) at $M = 2.01$ by relocating the canard surface until the root leading edge was coincident with the forebody apex. The results (fig. 10) indicate that moving the canard surface forward causes a slight reduction in longitudinal stability and an increase in the pitch-up tendency. The configuration with the forward canard surface also indicates a slight increase in lift-curve slope and a decrease in drag at high lift. This increase in lift and decrease in drag may result from a change in the wake effects of the canard flow field on the wing; however, the forward canard surface differed in section and thickness from the canard surface used in the normal position, and those differences may also contribute to the small changes in lift and drag.

The effects of canard size on the trimmed longitudinal characteristics for a constant center-of-gravity position (figs. 11 and 12) indicate that as the canard area is increased the variation of trim C_L with δ_c increases markedly. This increase would be reflected in higher

maneuverability and in increased altitude capability. Increasing the canard size generally indicates a slight increase in the trim lift-curve slope and an increase in maximum L/D. These results should be expected, however, since for a constant center-of-gravity position the static margin decreases with increase in canard area.

The effect of canard size on the trimmed longitudinal characteristics with a constant static margin for the delta-wing configuration at $M = 2.01$ is shown in figure 13. For this example, the center of gravity for the configuration with the smaller canard was shifted rearward approximately 10 percent so that the static margin was the same as for the configuration with the larger canard. With this more rearward center-of-gravity position, the configuration with the smaller canard indicates a considerable increase in the variation of trim C_L with δ_c (refer also to fig. 11(b)) while the maximum value of L/D is only slightly less than for the configuration having the larger canard.

A summary of the variations of $\partial C_m/\partial C_L$ and C_{m_δ} with canard volume coefficient $S_c l_c/S_w \bar{c}_w$ is presented in figure 14. The estimated variations were obtained by the method of reference 2 but do not include interference effects between the canard surfaces and the wings. In general, the experimentally determined variations of C_{m_δ} and $\partial C_m/\partial C_L$ with canard surface area are in good agreement with the estimated variations.

The effect of changing the canard volume coefficient by varying the canard longitudinal position l_c for the delta-wing configuration with one of the canard surfaces $(S_c/S_w = 0.062)$ at $\delta_c = 0^\circ$ is shown in figure 14(b). The results indicate only a small variation in $\partial C_m/\partial C_L$ with canard volume coefficient. This result might be expected since the carry-over lift effects of the canard surface on the body would become smaller as the canard surface is moved to the forward position.

Some additional variations of $\partial C_m/\partial C_L$ with canard volume coefficient are included in figure 14 wherein l_c is changed by means of varying the center-of-gravity position for a given canard area and position. This method of varying the stability level is considerably more effective than either varying the canard area or the canard position because varying the center-of-gravity position serves a twofold purpose in changing the stability level; that is, as the center of gravity is moved rearward, the stabilizing influence of the wing is reduced, whereas the destabilizing influence of the canard is increased.

Lateral Characteristics

It should be kept in mind that changes in the size of the canard surface or in the center-of-gravity position may affect the directional-stability characteristics; hence any configuration that appears desirable from a longitudinal-control standpoint should also be examined from a directional-stability standpoint.

The effects of canard size on the sideslip characteristics for $\delta_c = 0$ at $M = 2.01$ (fig. 15) are relatively small for both configurations; hence, the improvements in the longitudinal characteristics provided by the larger canard surfaces are obtained at no expense to the lateral and directional characteristics. The effects of the center-of-gravity position on C_{n_β}, on the other hand, become quite large, as indicated in figure 16 for the delta-wing configuration with the larger canard surface at $M = 2.01$. (A similar effect would be indicated for the other canard surfaces.) The change in C_{n_β} with α for a shift of $\pm 0.1\bar{c}_w$ in the center-of-gravity position is shown since this is approximately the shift that would be required to provide equal static margins for the configuration with the smallest and the largest canard surfaces. (See fig. 14(b).) In order for the configuration with the small canard surface to have the same static margin as the configuration with the large canard surface, therefore, it would be necessary to shift the center-of-gravity position rearward 10 percent ($\Delta x/\bar{c}_w = -0.1$) with a resultant loss in directional stability. Accordingly, in order for the configuration with the large canard surface to have the same static margin as the configuration with the small canard surface, it would be necessary to shift the center-of-gravity position forward 10 percent ($\Delta x/\bar{c}_w = 0.1$) with a resultant increase in directional stability.

Whereas variations in the center-of-gravity position provide an effective means of altering the longitudinal trim characteristics, these variations may be limited by other factors such as directional stability.

SUMMARY OF RESULTS

An investigation has been made in the Langley 4- by 4-foot supersonic pressure tunnel at Mach numbers of 1.41 and 2.01 to determine the effects of canard surface size on the aerodynamic characteristics of a generalized canard airplane configuration equipped either with a delta-plan-form wing or with a trapezoidal-plan-form wing. The results of the investigation indicated the following:

1. In general, the experimentally determined variations of control effectiveness C_{m_δ} and longitudinal stability $\partial C_m/\partial C_L$ with canard surface area were in good agreement with estimated variations.

2. For a constant center-of-gravity position, the maximum trimmed lift-drag ratio increased with increasing canard size because of decreased stability. For a constant static margin, however, the maximum lift-drag ratio was only slightly less with the smallest canard than with the largest canard.

3. The effects of canard size on the sideslip derivatives were relatively small. However, variations in the center-of-gravity position that are effective in altering the longitudinal trim characteristics may be limited by the directional-stability requirements.

Langley Aeronautical Laboratory,
National Advisory Committee for Aeronautics,
Langley Field, Va., December 9, 1957.

REFERENCES

1. Driver, Cornelius: Longitudinal and Lateral Stability and Control Characteristics of Two Canard Airplane Configurations at Mach Numbers of 1.41 and 2.01. NACA RM L56L19, 1957.

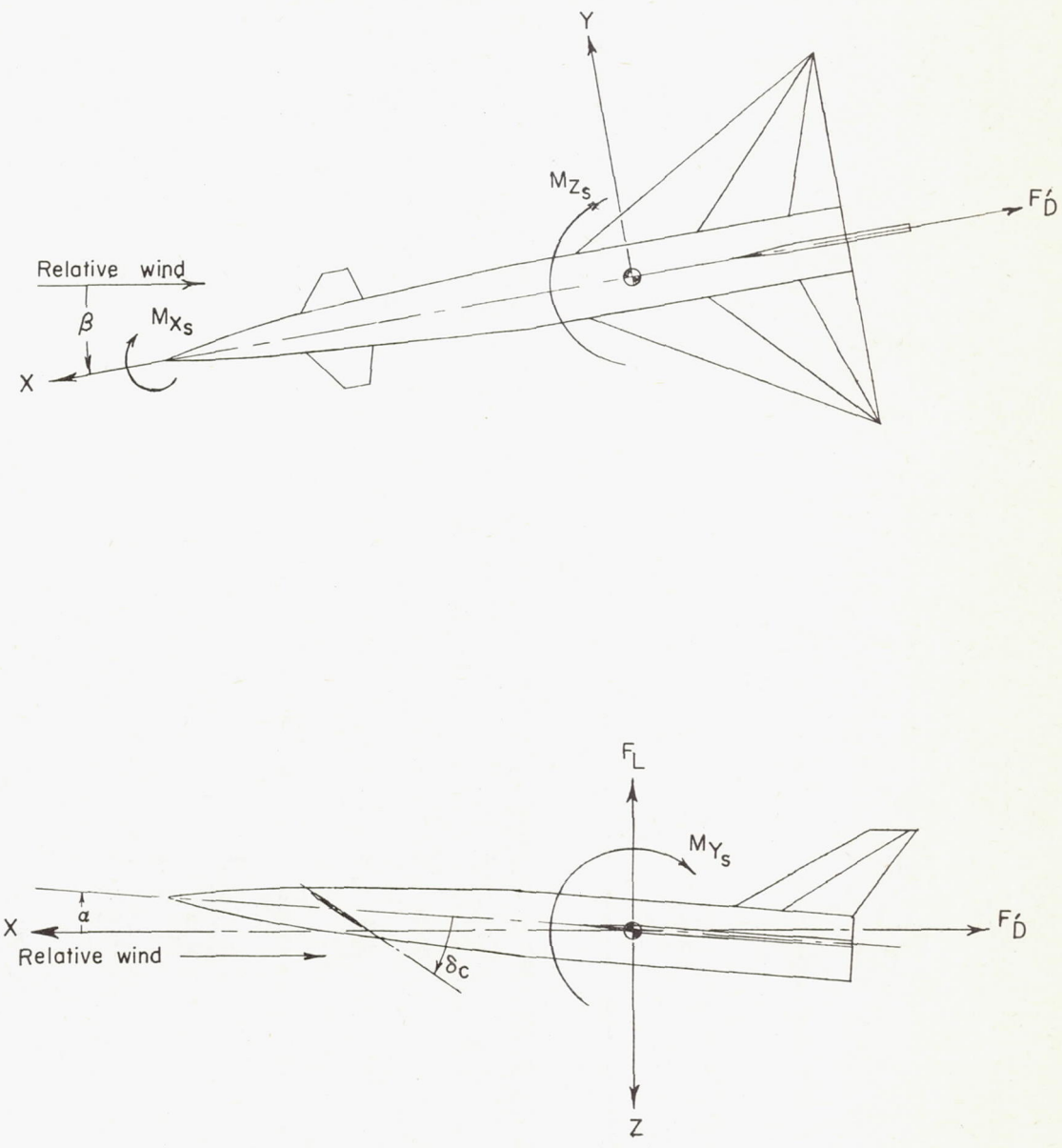
2. Nielsen, Jack N., Kaattari, George E., and Anastasio, Robert F.: A Method for Calculating the Lift and Center of Pressure of Wing-Body-Tail Combinations at Subsonic, Transonic, and Supersonic Speeds. NACA RM A53G08, 1953.

TABLE I.- GEOMETRIC CHARACTERISTICS OF MODEL

Body:	
Maximum diameter, in.	3.50
Length, in.	37.00
Base area, sq in.	9.582
Fineness ratio	10.57
Trapezoidal Wing:	
Span, in.	25.72
Chord at body-wing intersection, in.	13.25
Area, sq ft	1.53
Aspect	3
Taper ratio	0.143
Thickness ratio	0.04
Mean geometric chord, in.	10.184
Sweep angle of leading edge	38° 40'
Sweep angle of 80-percent-chord line, deg	0
Sweep angle of trailing edge	-11°-18'
Leading-edge half-angle, normal to L.E., deg	5
Trailing-edge half-angle, normal to T.E., deg	5
Delta Wing:	
Span, in.	22.56
Chord at body-wing intersection, in.	16.51
Mean geometric chord, in.	13.027
Area, sq ft	1.53
Aspect ratio	2.31
Taper ratio	0
Thickness ratio	0.036
Sweep angle of leading edge, deg	60
Leading-edge half-angle, normal to L.E., deg	5
Trailing-edge half-angle, normal to T.E., deg	5
Vertical Tail:	
Area, exposed, sq ft	0.279
Span, exposed, in.	4.25
Aspect ratio	0.439
Sweep of leading edge, deg	80
Section	3/16 in. wedge slab
Leading-edge half-angle, normal to L.E., deg	5
Ventral Fins:	
Area, each fin, sq ft	0.13
Span, exposed, in.	2.25
Aspect ratio	0.271
Sweep leading edge, deg	60
Sweep trailing edge, deg	-77.5
Leading-edge half-angle, normal to L.E., deg	5
Trailing-edge half-angle, normal to T.E., deg	5

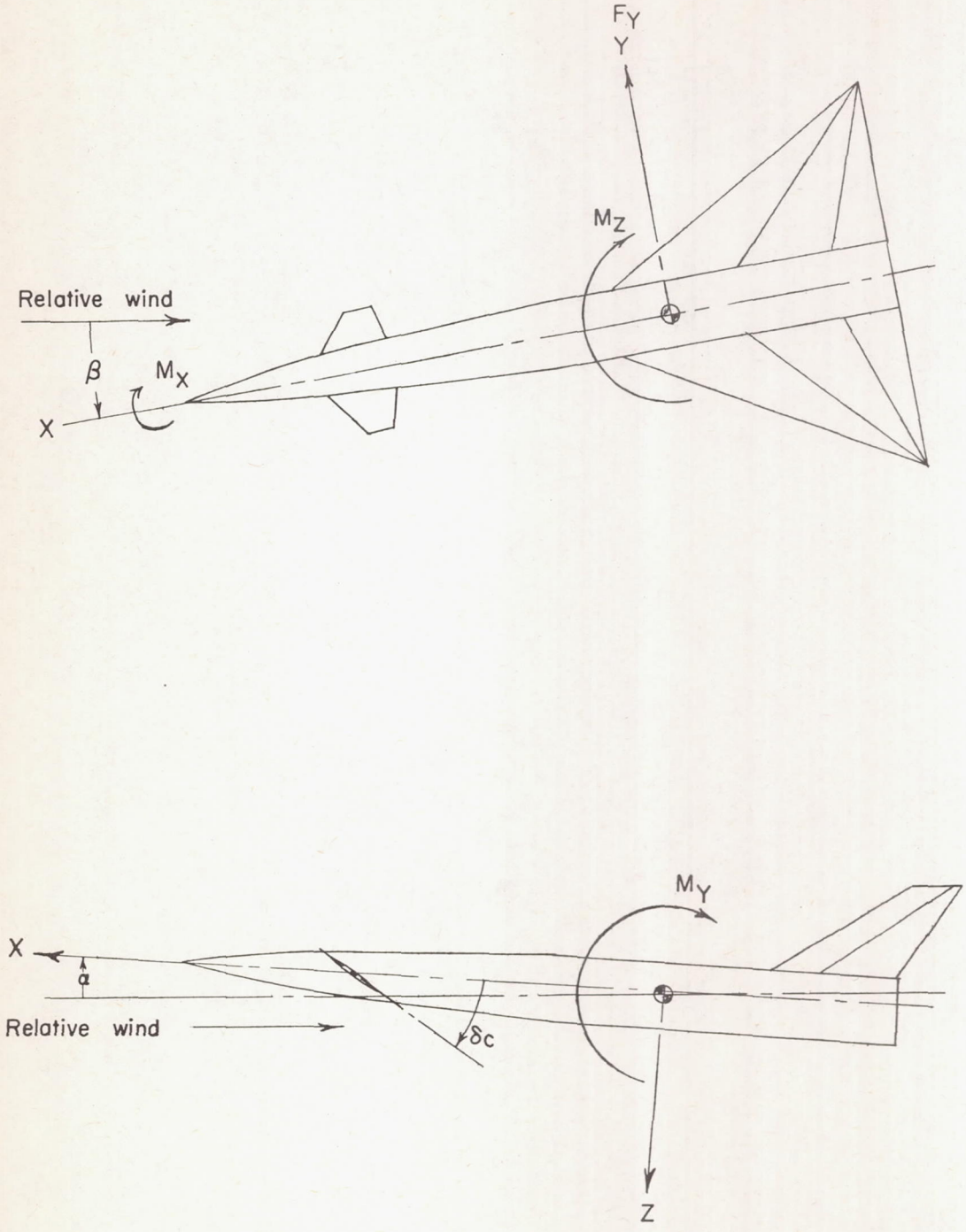
TABLE II.- BODY COORDINATES

Body station	Radius
0	0
.297	.076
.627	.156
.956	.233
1.285	.307
1.615	.378
1.945	.445
2.275	.509
2.605	.573
2.936	.627
3.267	.682
3.598	.732
3.929	.780
4.260	.824
4.592	.865
4.923	.903
5.255	.940
5.587	.968
5.920	.996
6.252	1.020
6.583	1.042 } Conical
18.648	1.75 } section
37.000	1.75



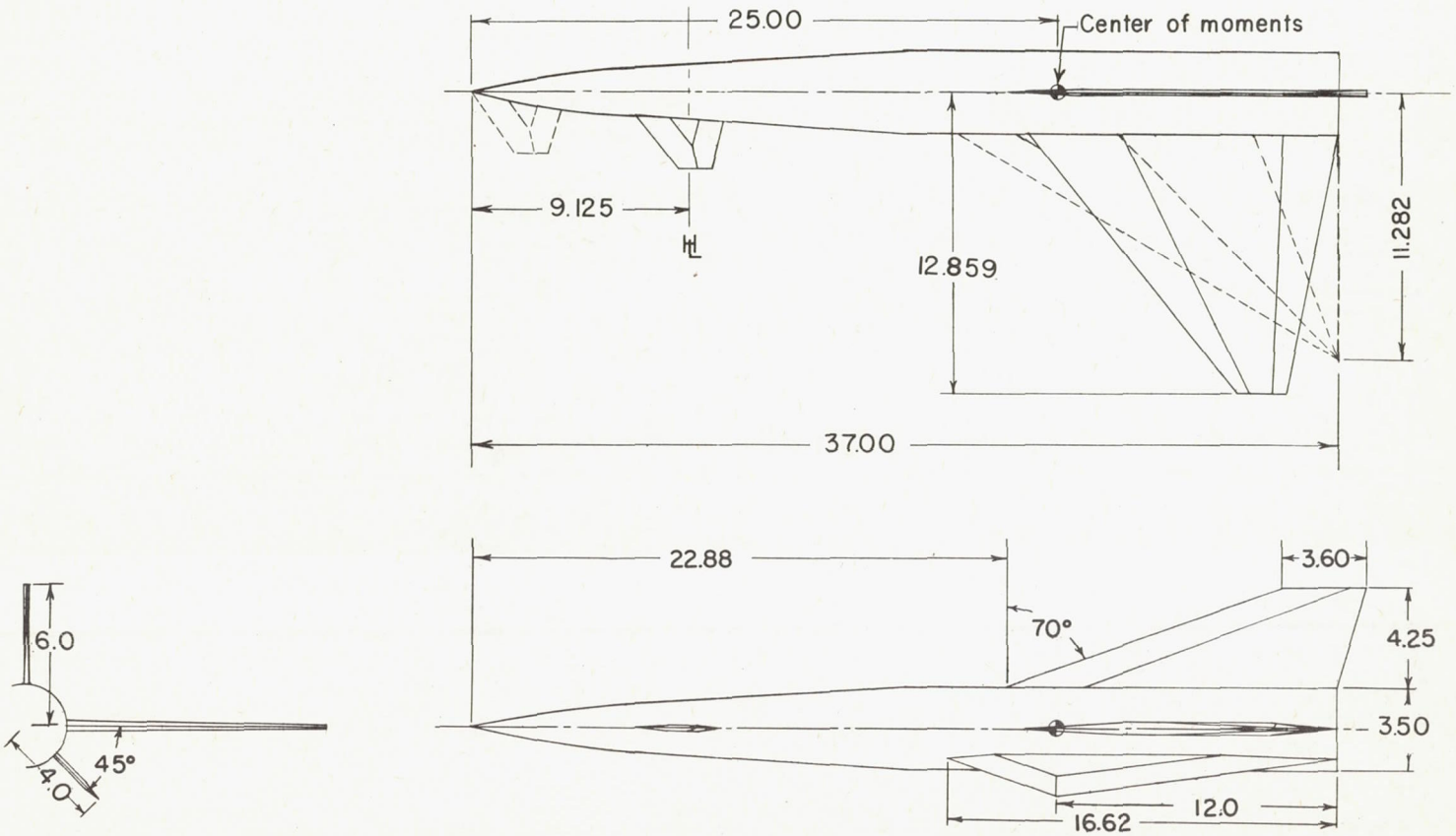
(a) Stability axis.

Figure 1.- Axes systems. (Arrows indicate positive directions.)



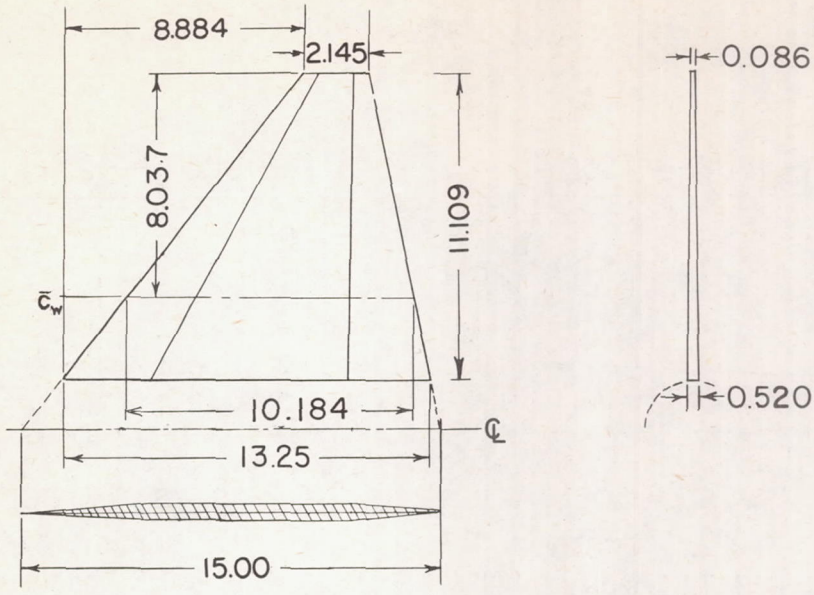
(b) Body axis.

Figure 1.- Concluded.

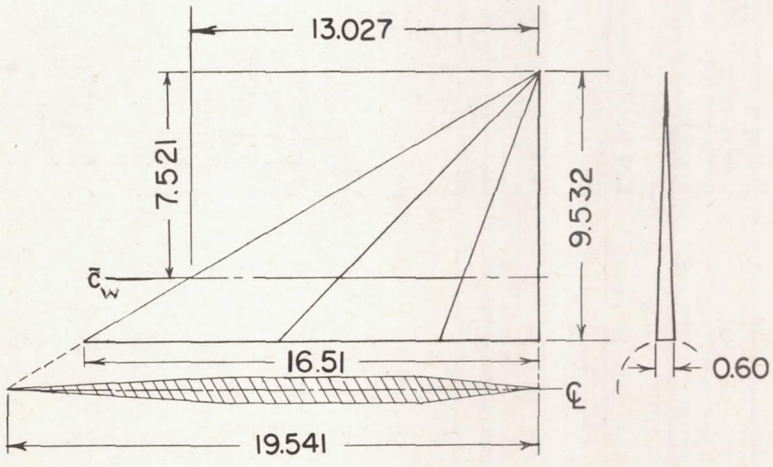


(a) Three-view drawing of model arrangement.

Figure 2.- Details of generalized canard airplane model.



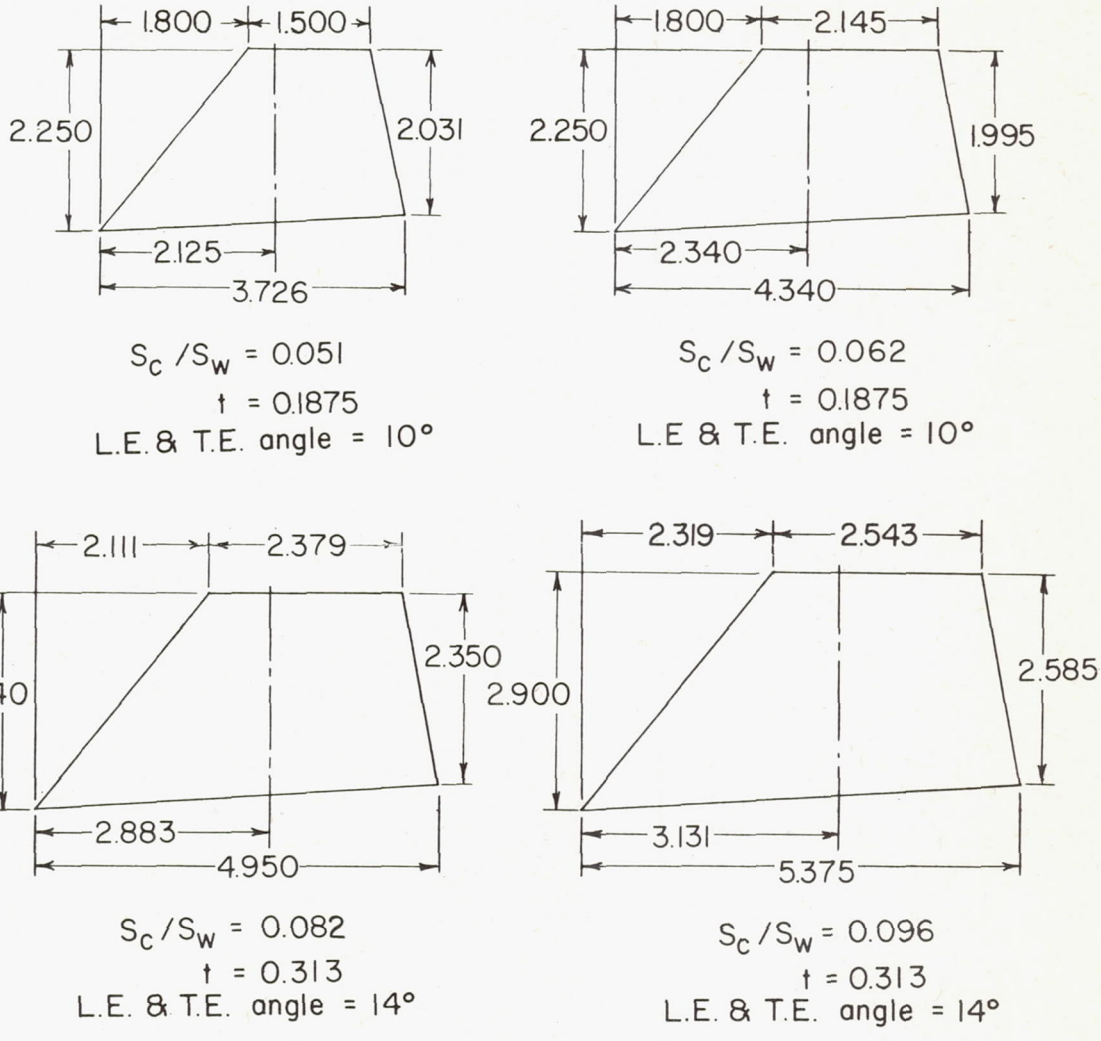
Trapezoidal wing ($\Lambda_{.80c}=0°$)



60° delta wing

(b) Details of wings.

Figure 2.- Continued.



(c) Details of canard control surfaces.

Figure 2.- Concluded.

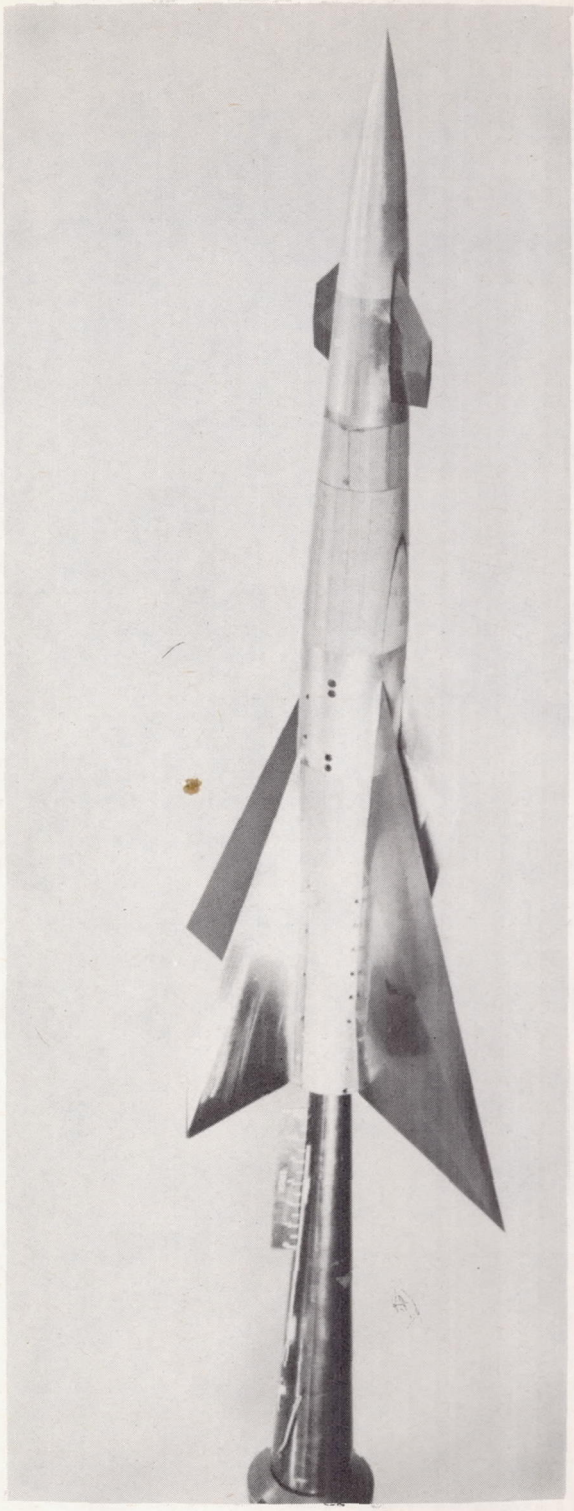
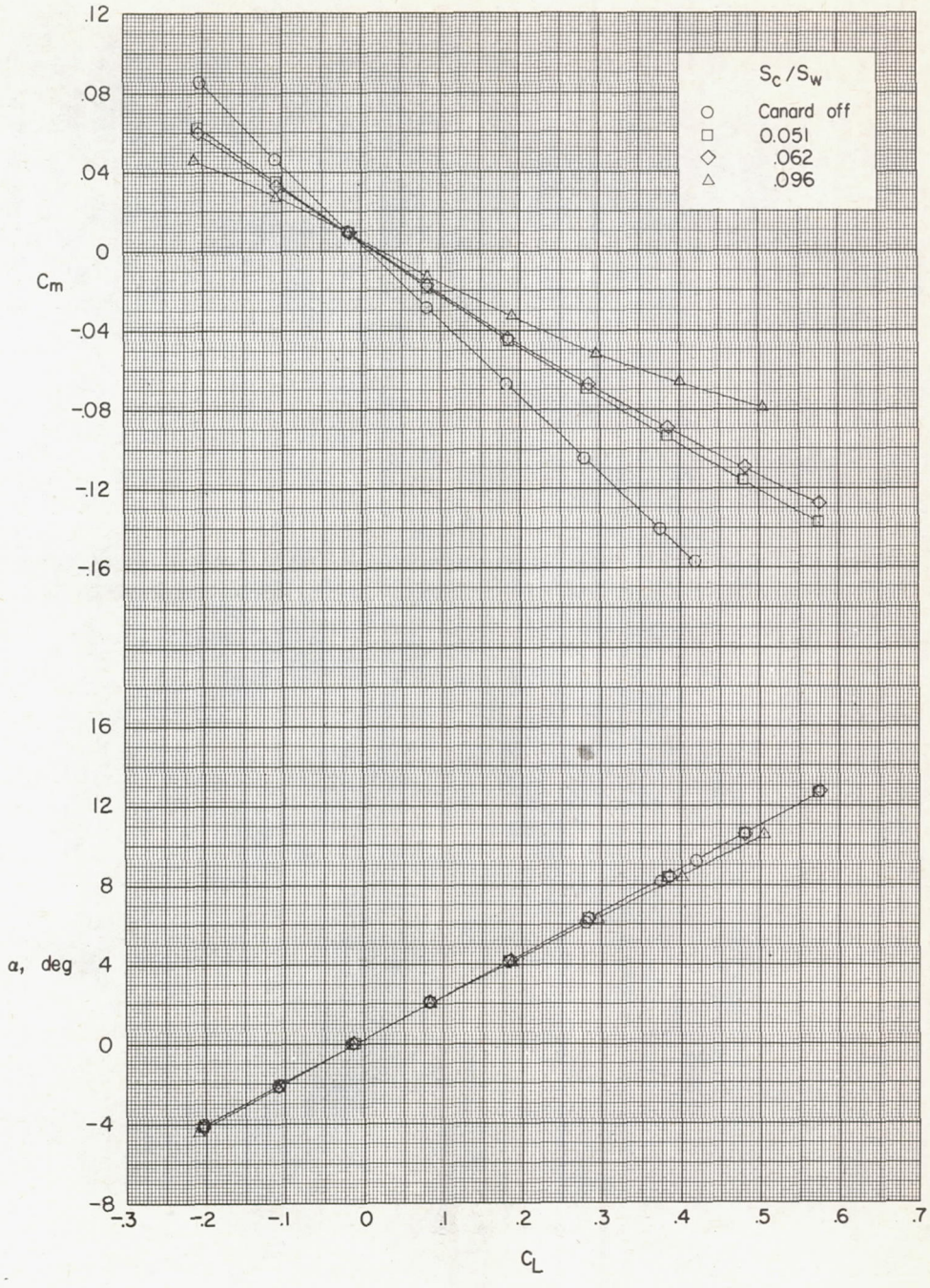
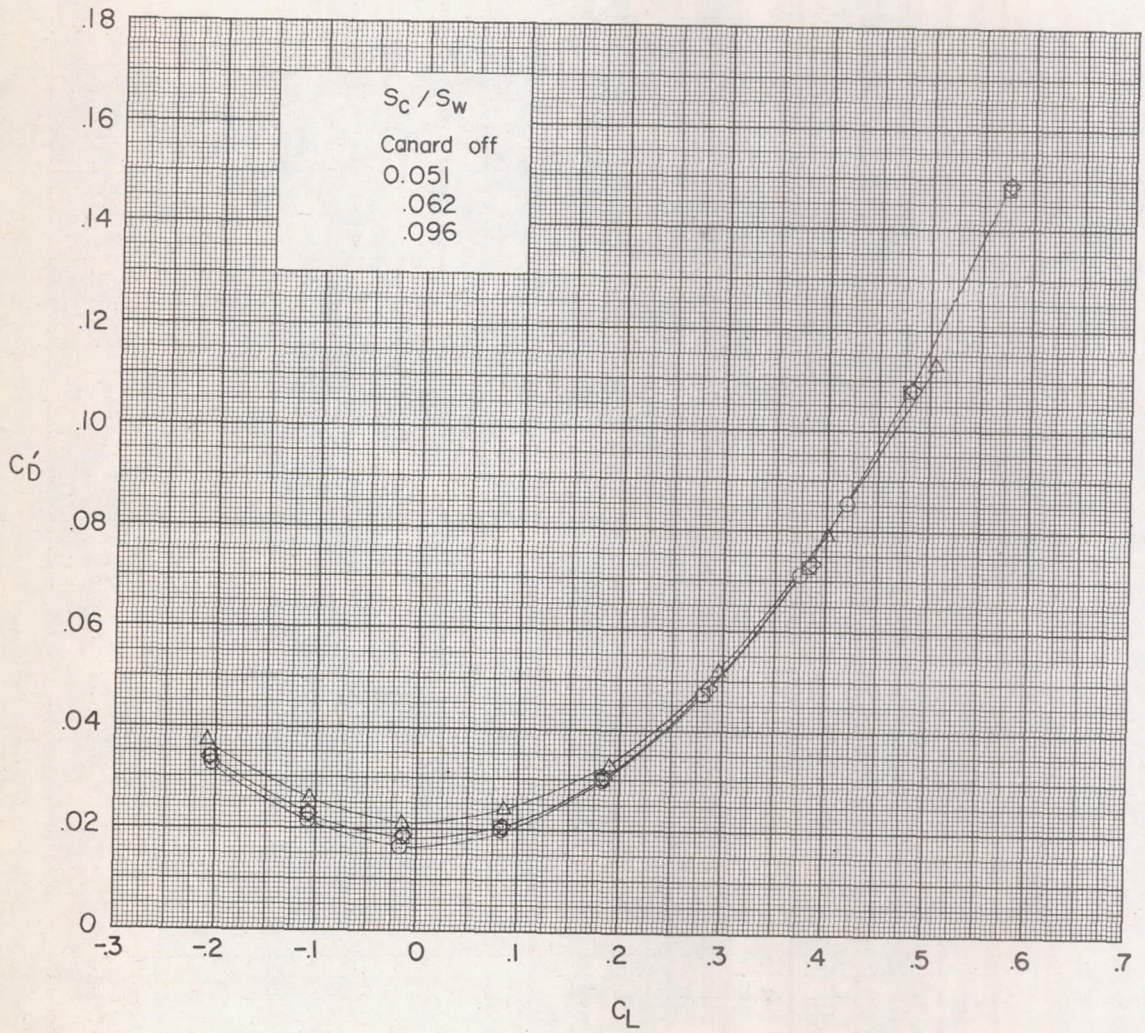


Figure 3.- Photograph of model with delta wing. L-94460



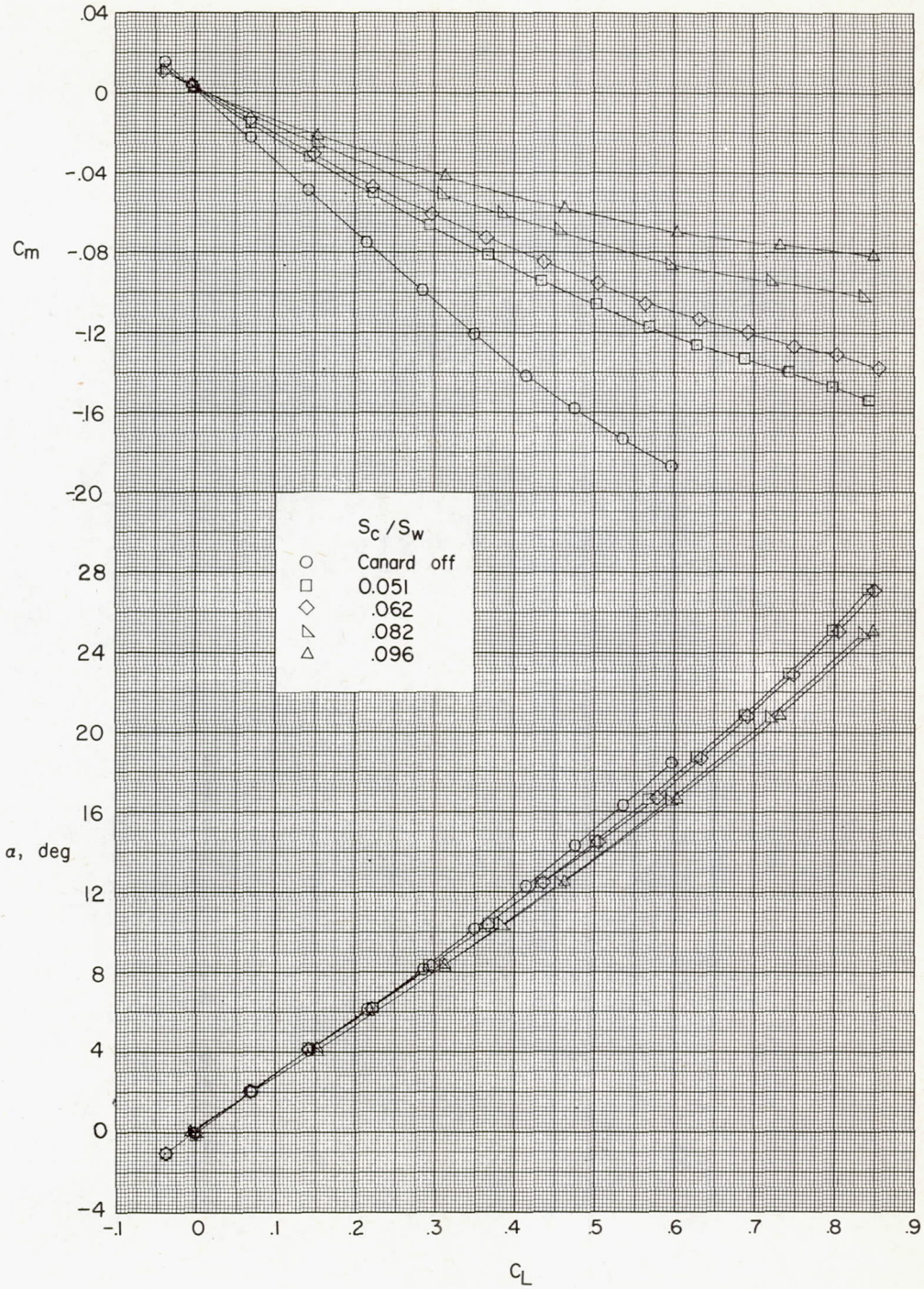
(a) M = 1.41.

Figure 4.- Effect of canard size on aerodynamic characteristics in pitch. Delta wing; $\delta_c = 0^o$.



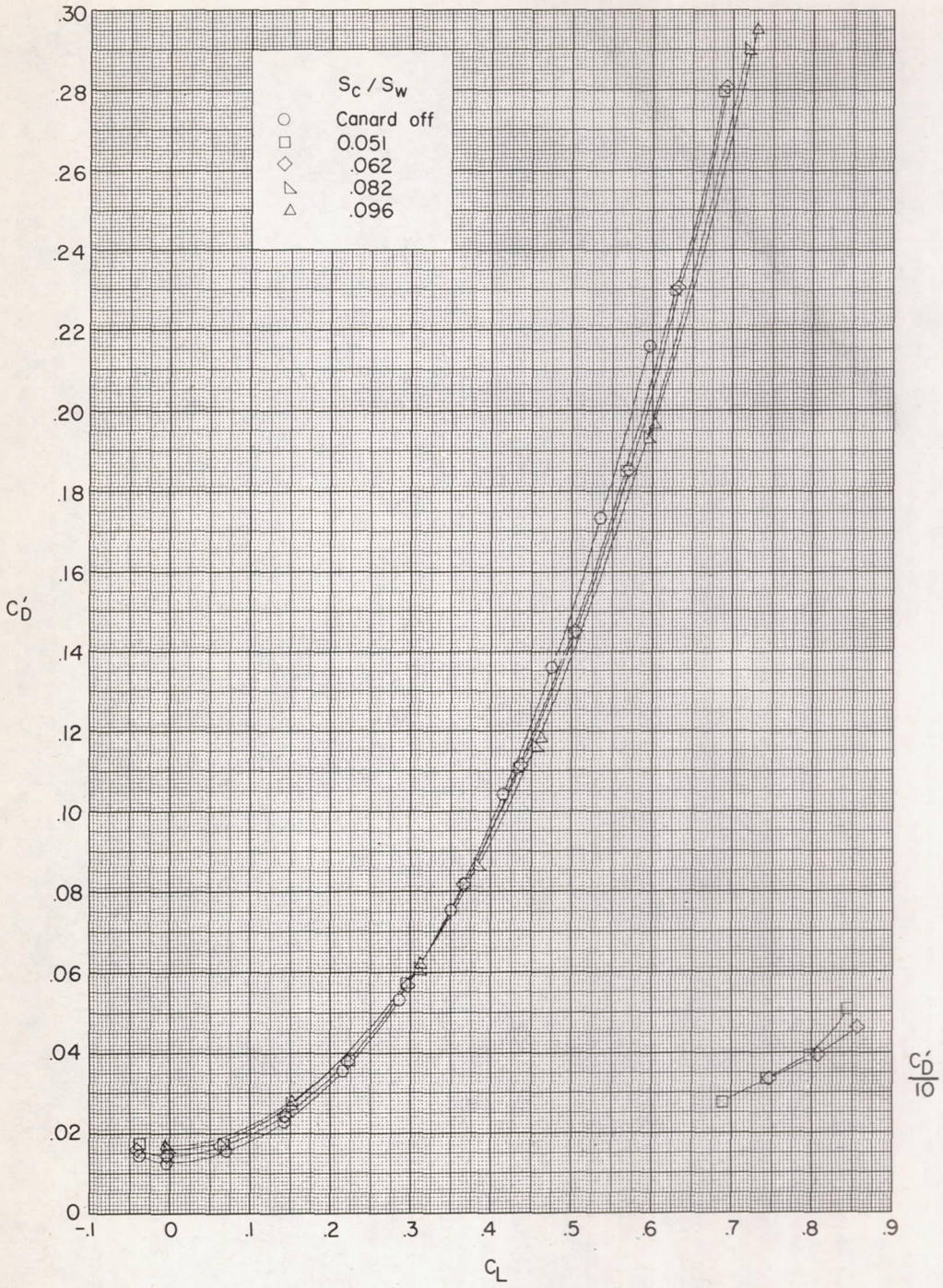
(a) Concluded.

Figure 4.- Continued.



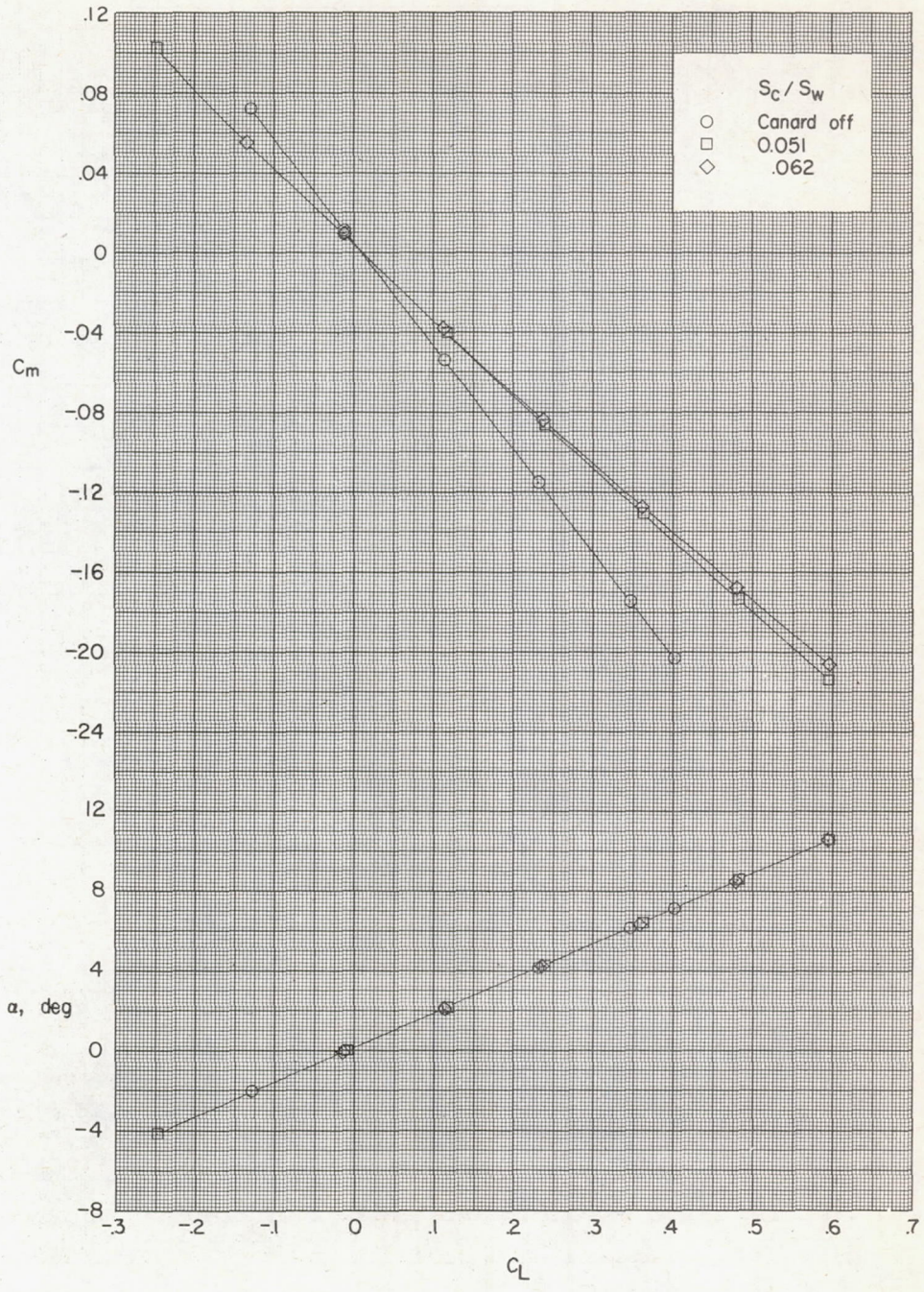
(b) M = 2.01.

Figure 4.- Continued.



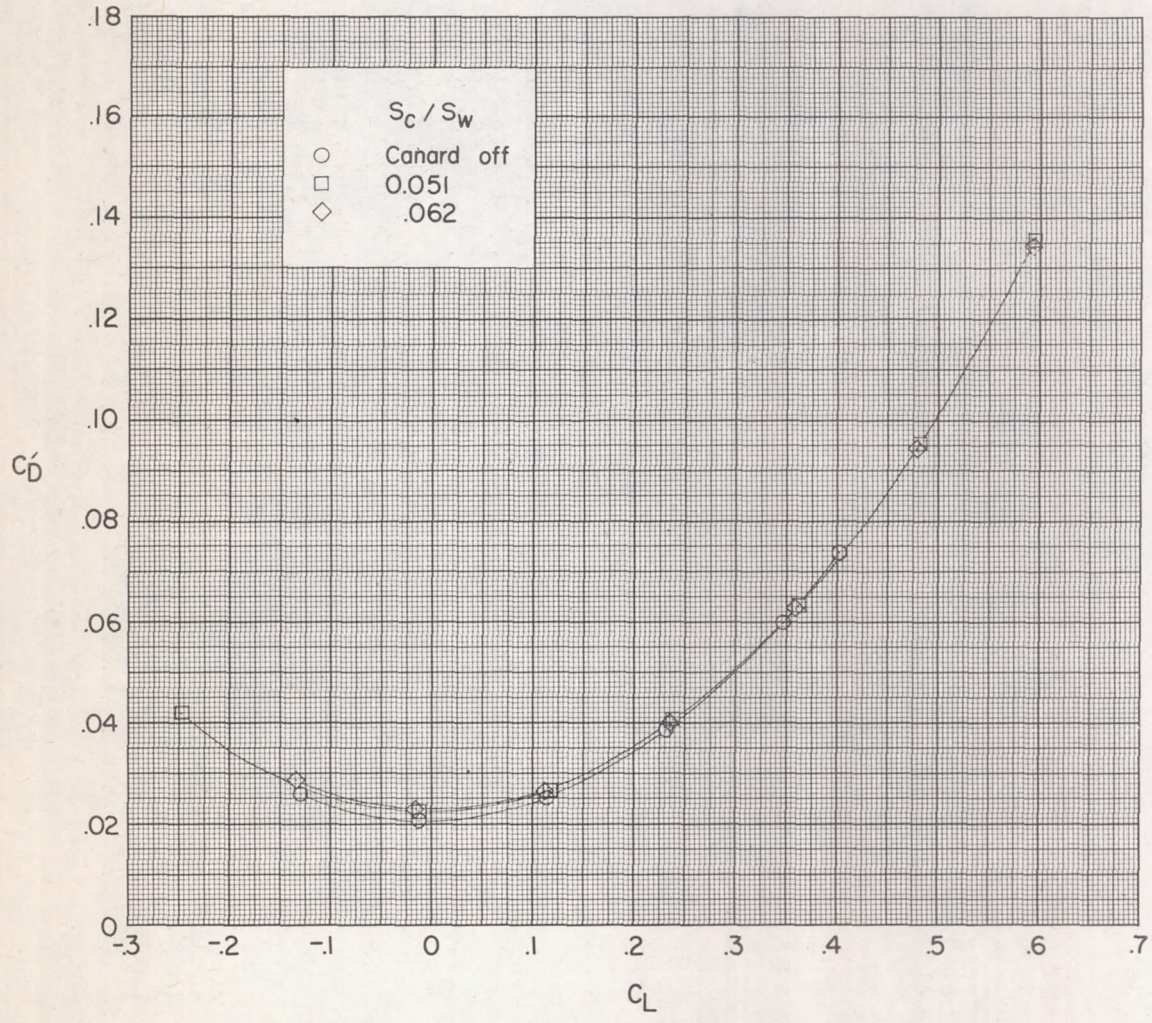
(b) Concluded.

Figure 4.- Concluded.



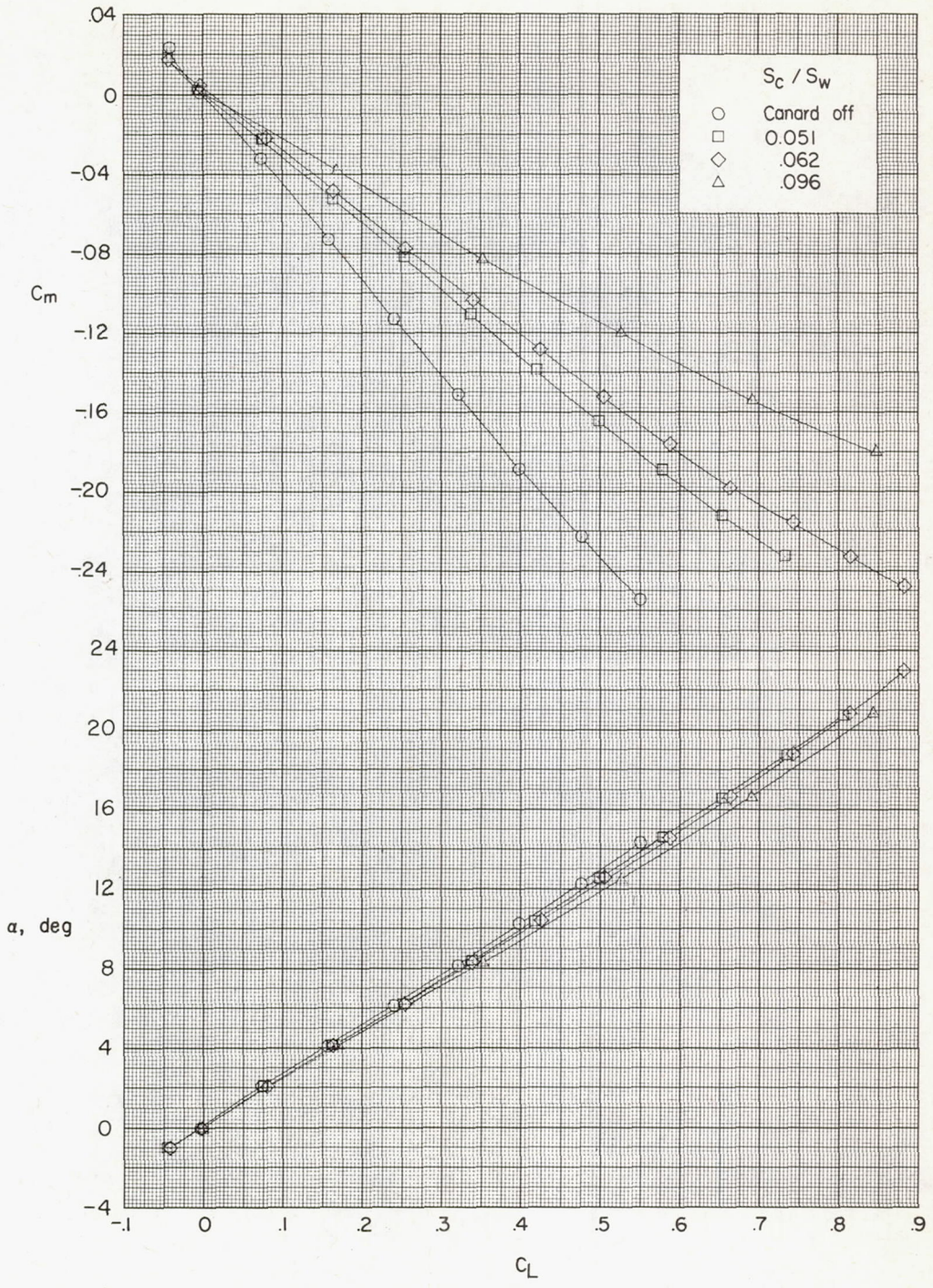
(a) M = 1.41.

Figure 5.- Effect of canard size on aerodynamic characteristics in pitch. Trapezoidal wing; $\delta_c = 0^o$.



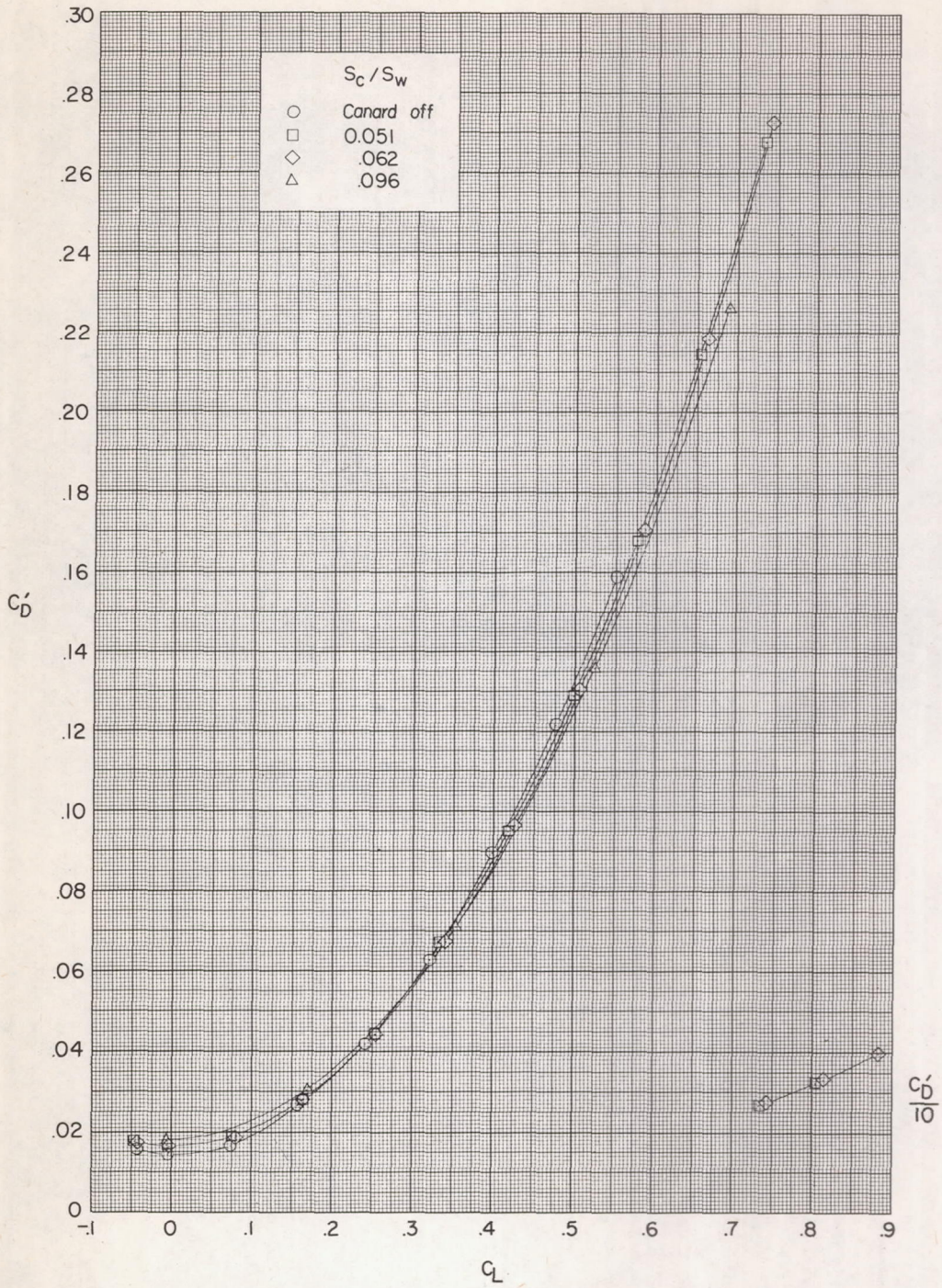
(a) Concluded.

Figure 5.- Continued.



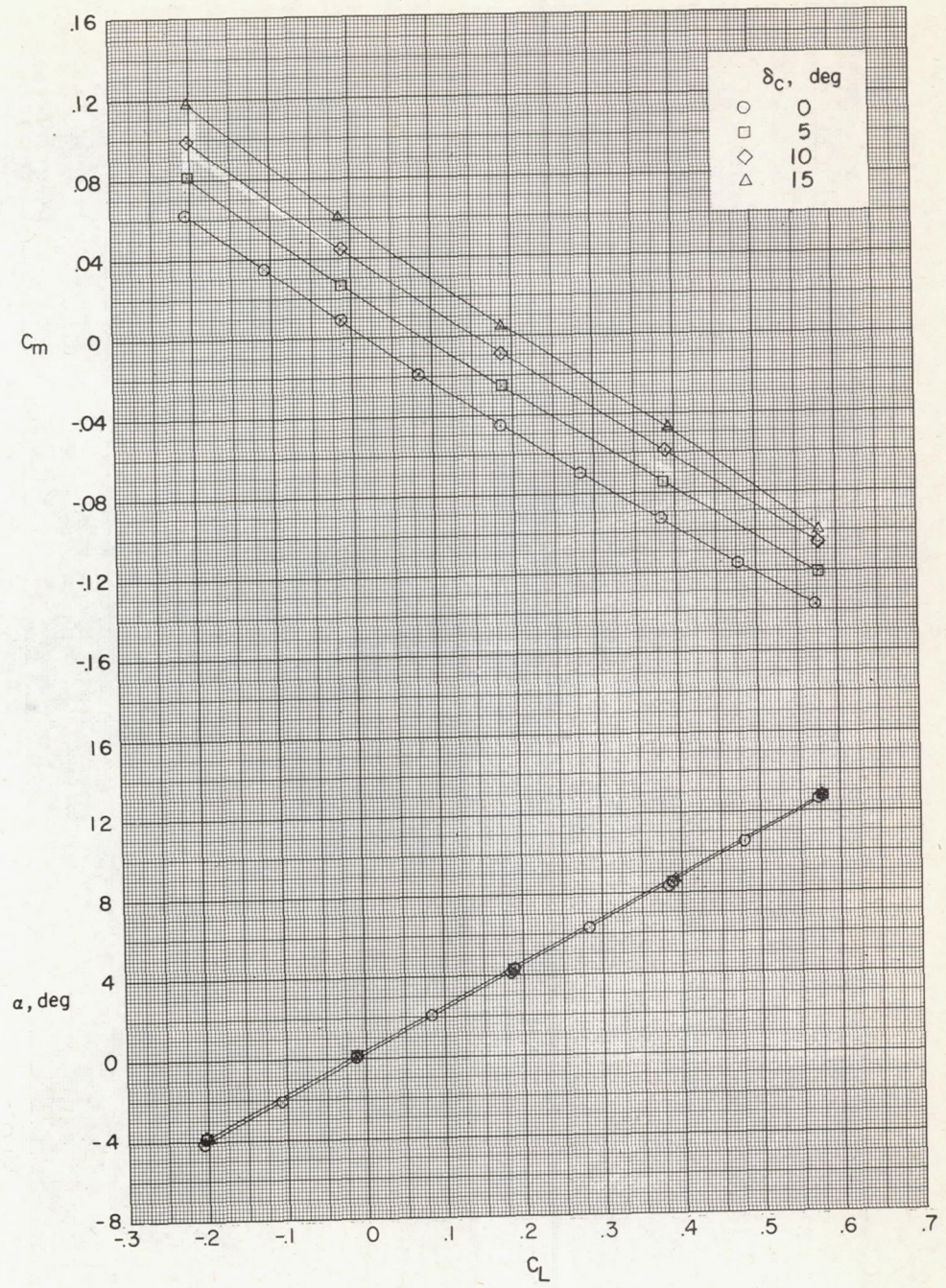
(b) M = 2.01.

Figure 5.- Continued.



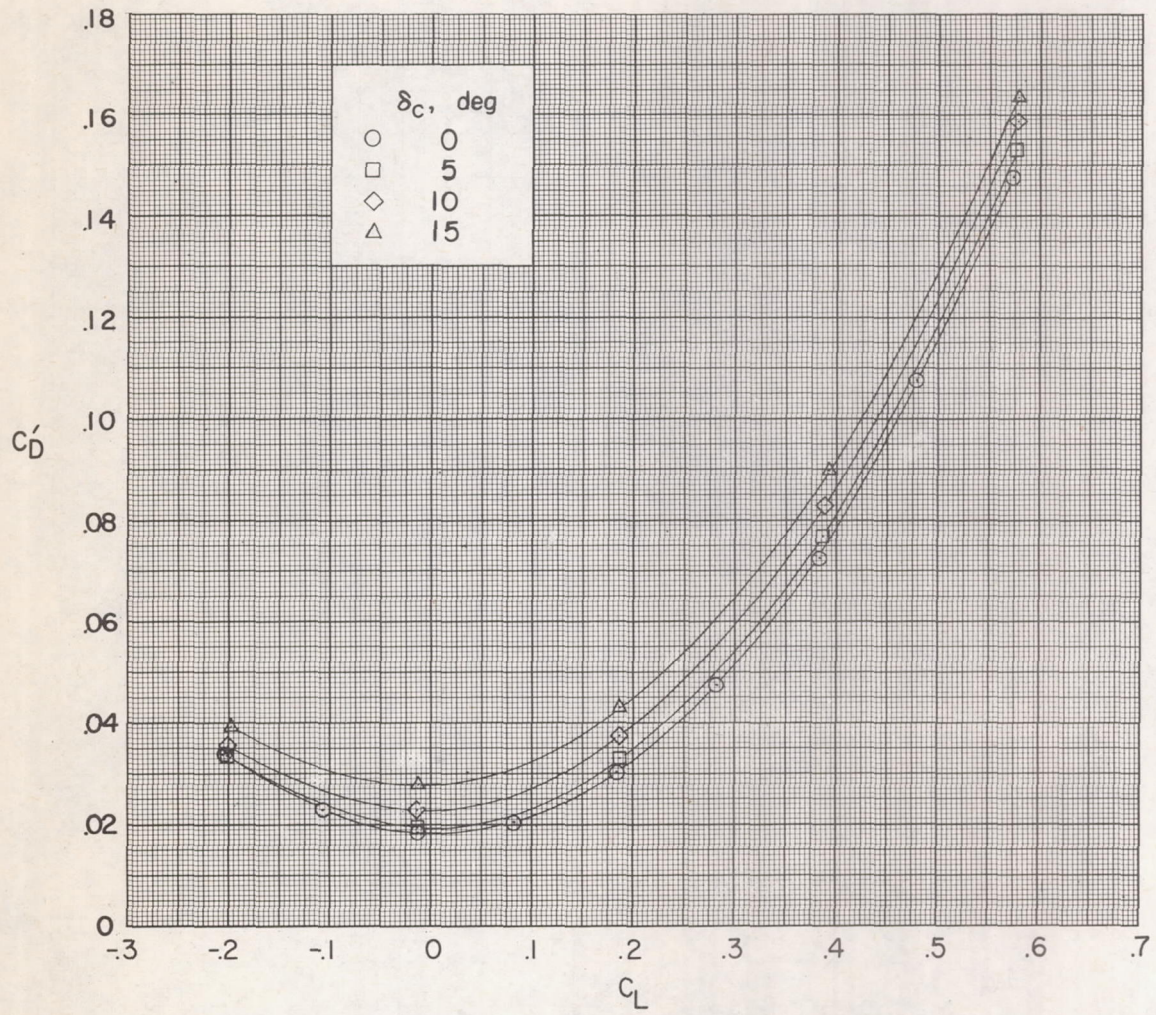
(b) Concluded.

Figure 5.- Concluded.



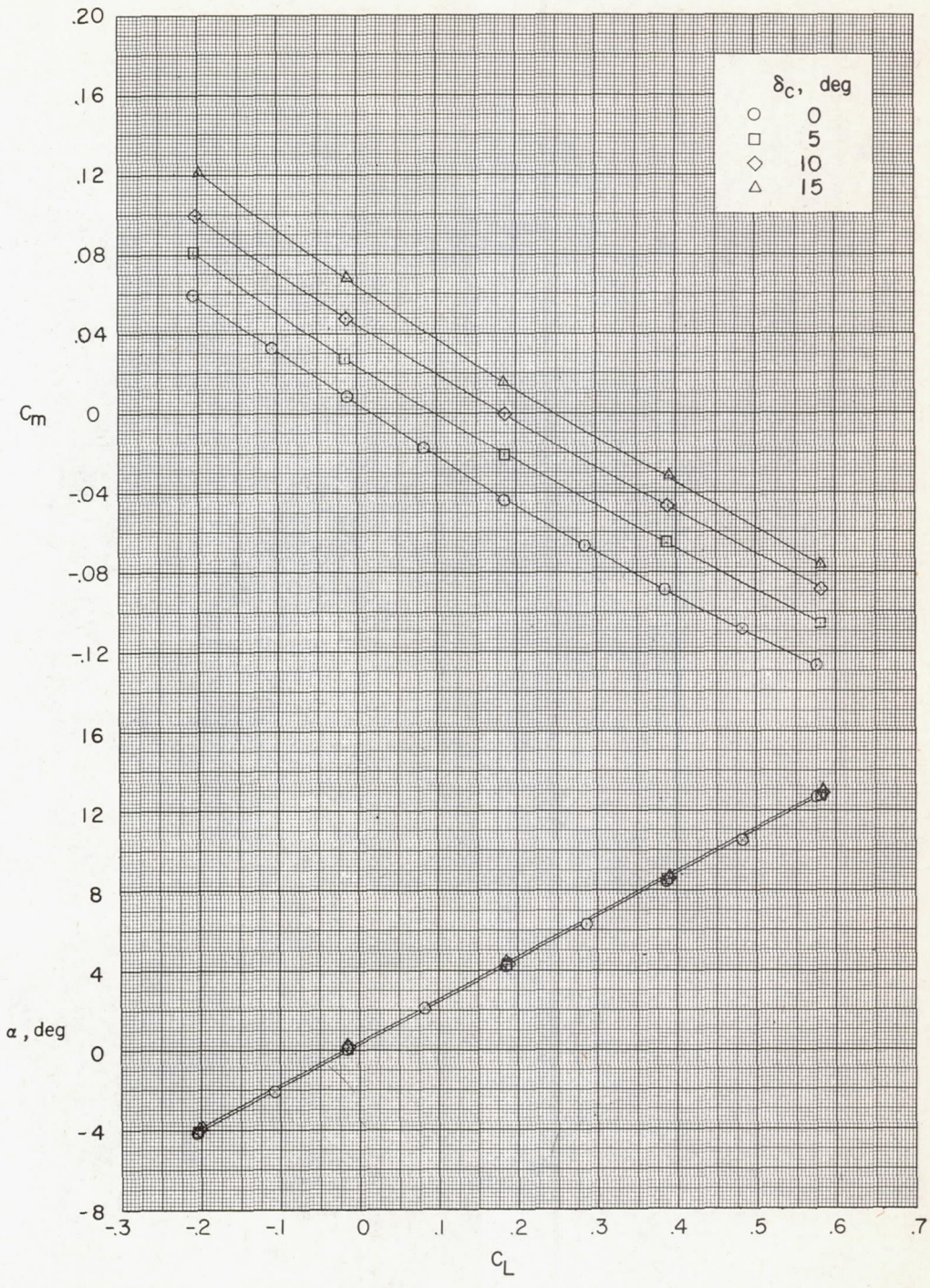
(a) $S_c/S_w = 0.051$.

Figure 6.- The aerodynamic characteristics in pitch of the configuration with the delta wing. M = 1.41.



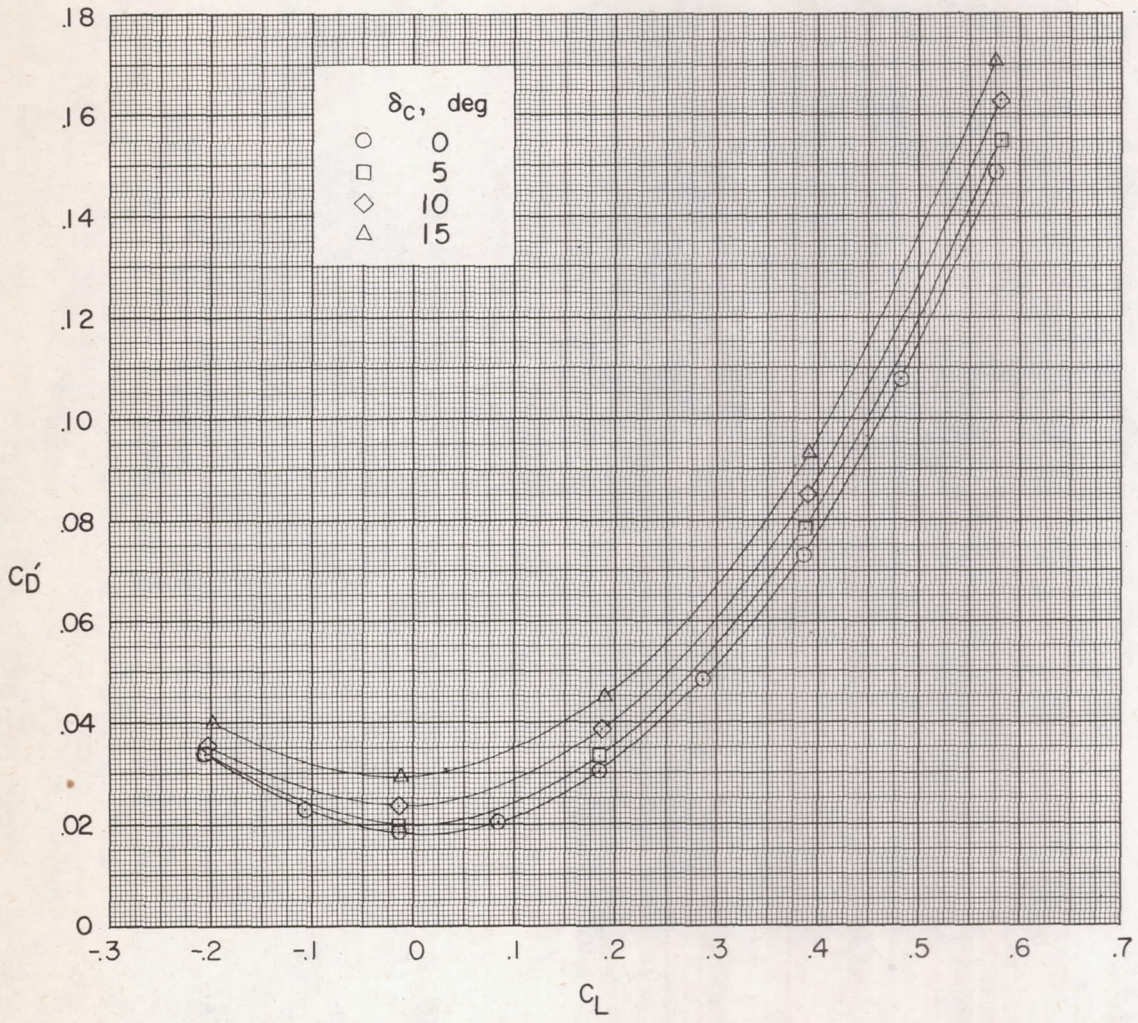
(a) Concluded.

Figure 6.- Continued.



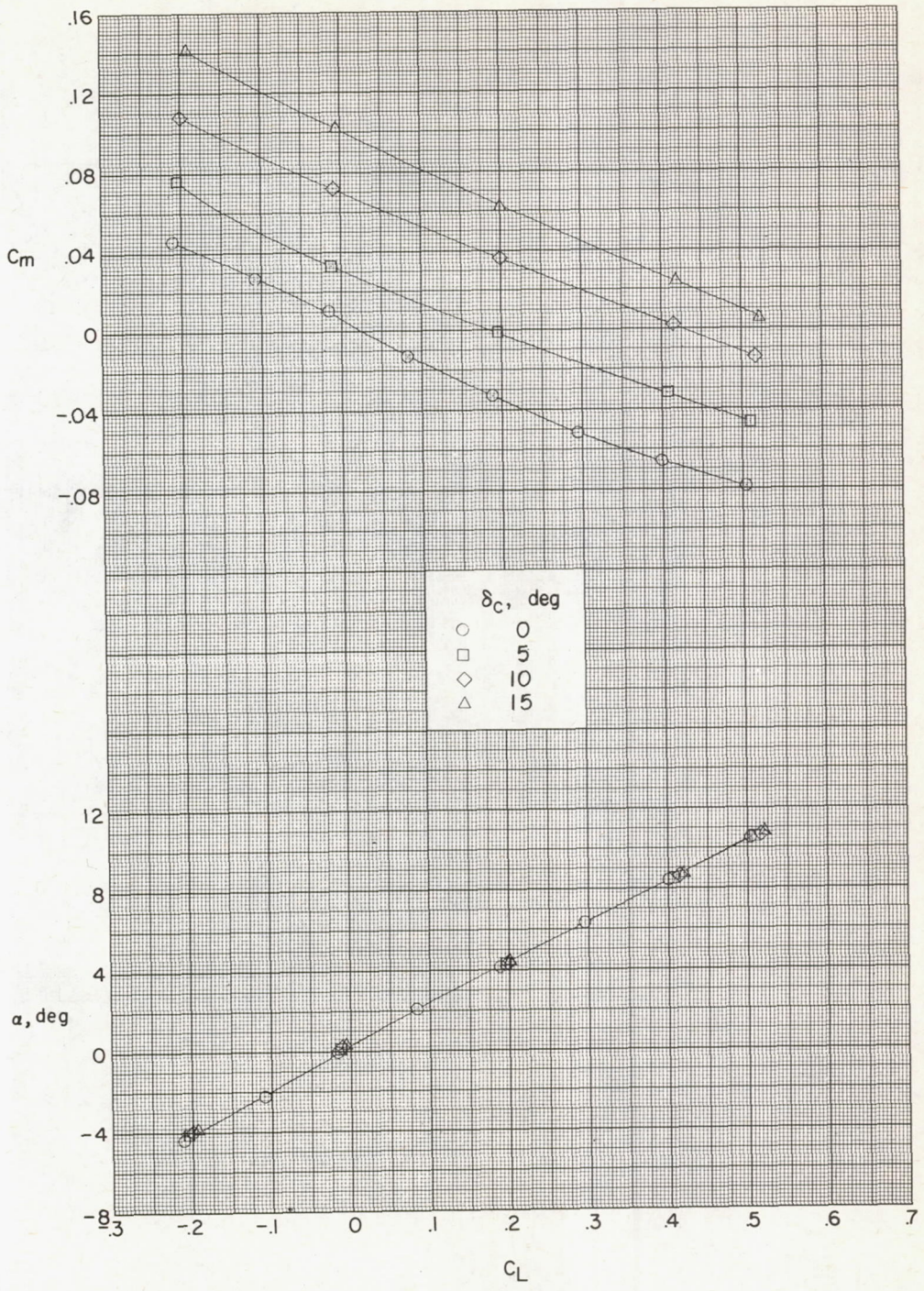
(b) $S_c/S_w = 0.062$.

Figure 6.- Continued.



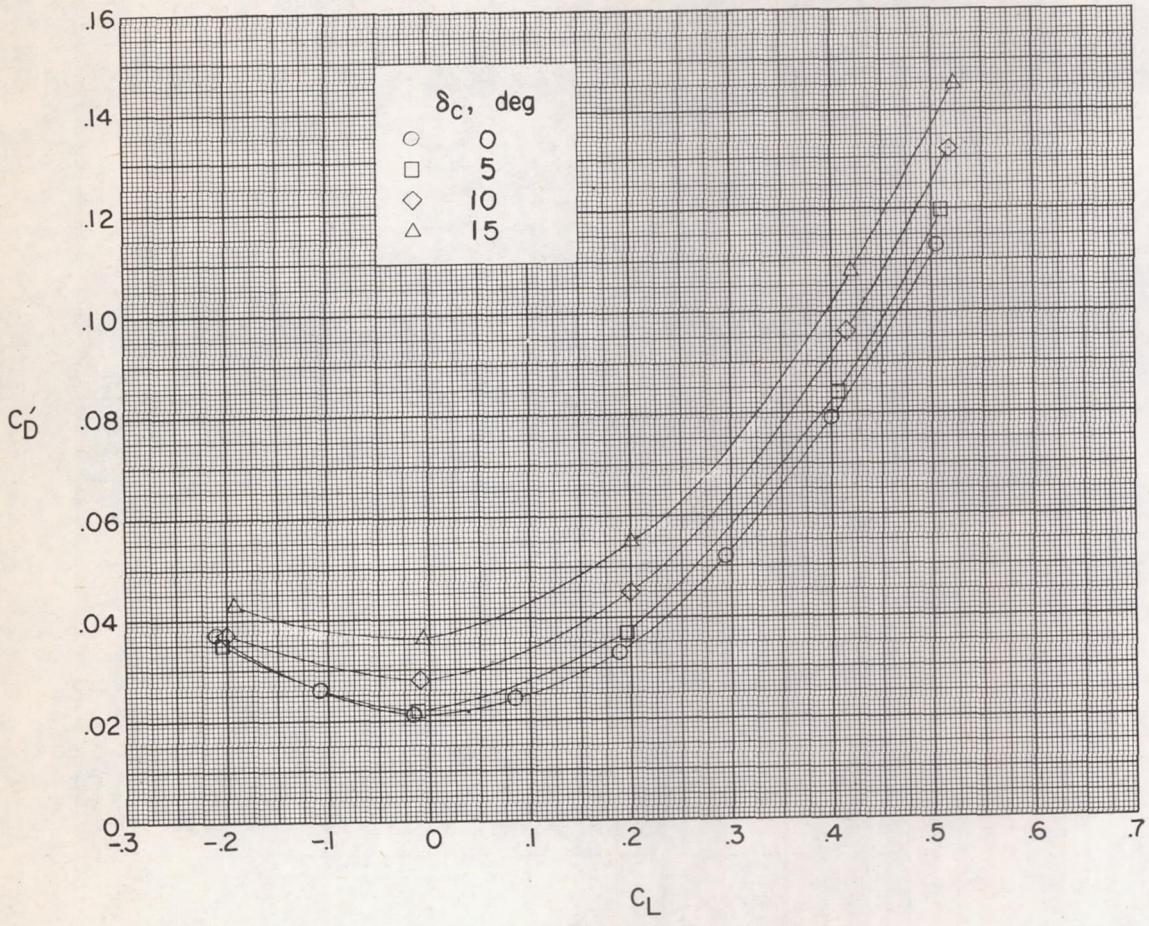
(b) Concluded.

Figure 6.- Continued.



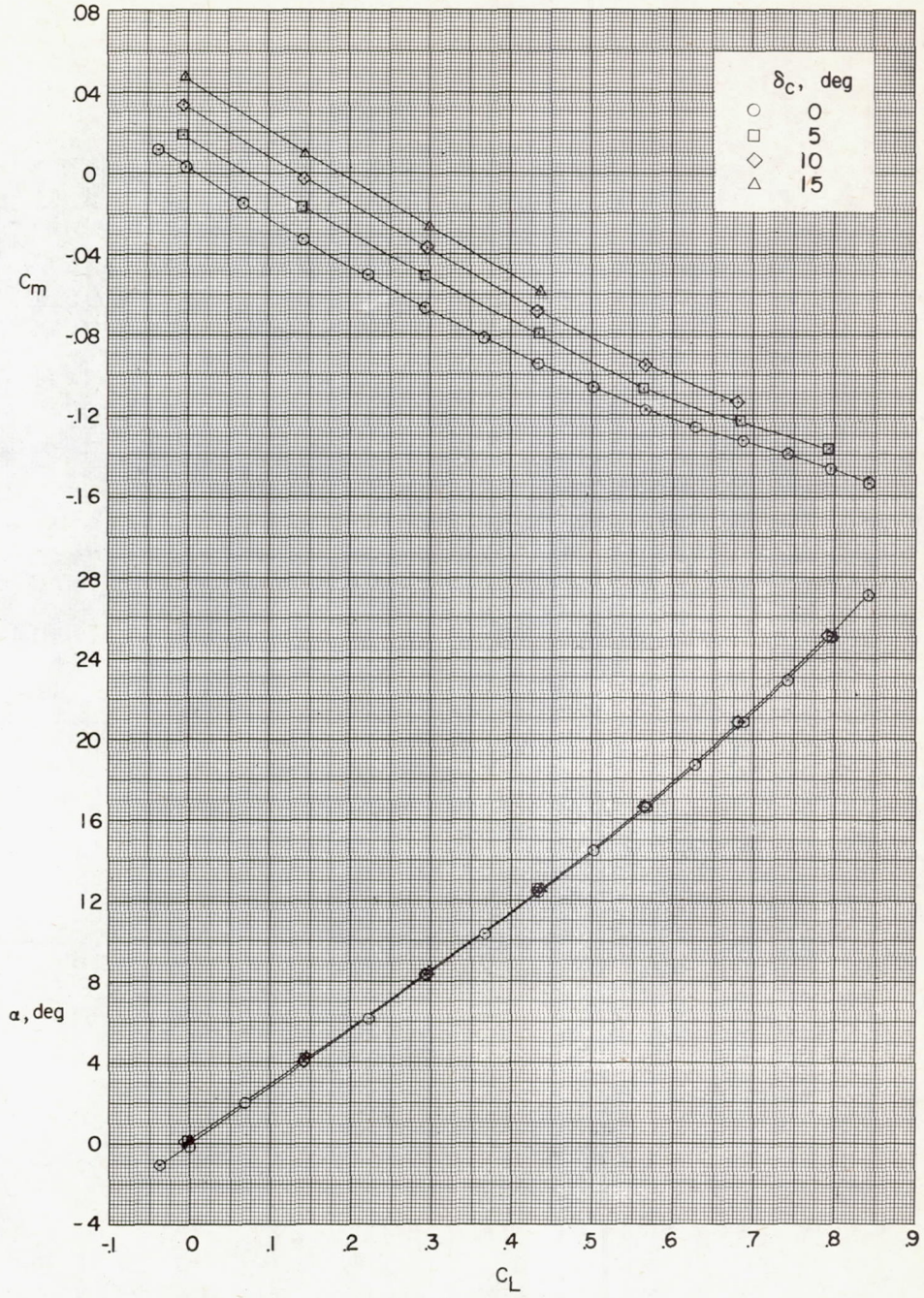
(c) $S_c/S_W = 0.096$.

Figure 6.- Continued.



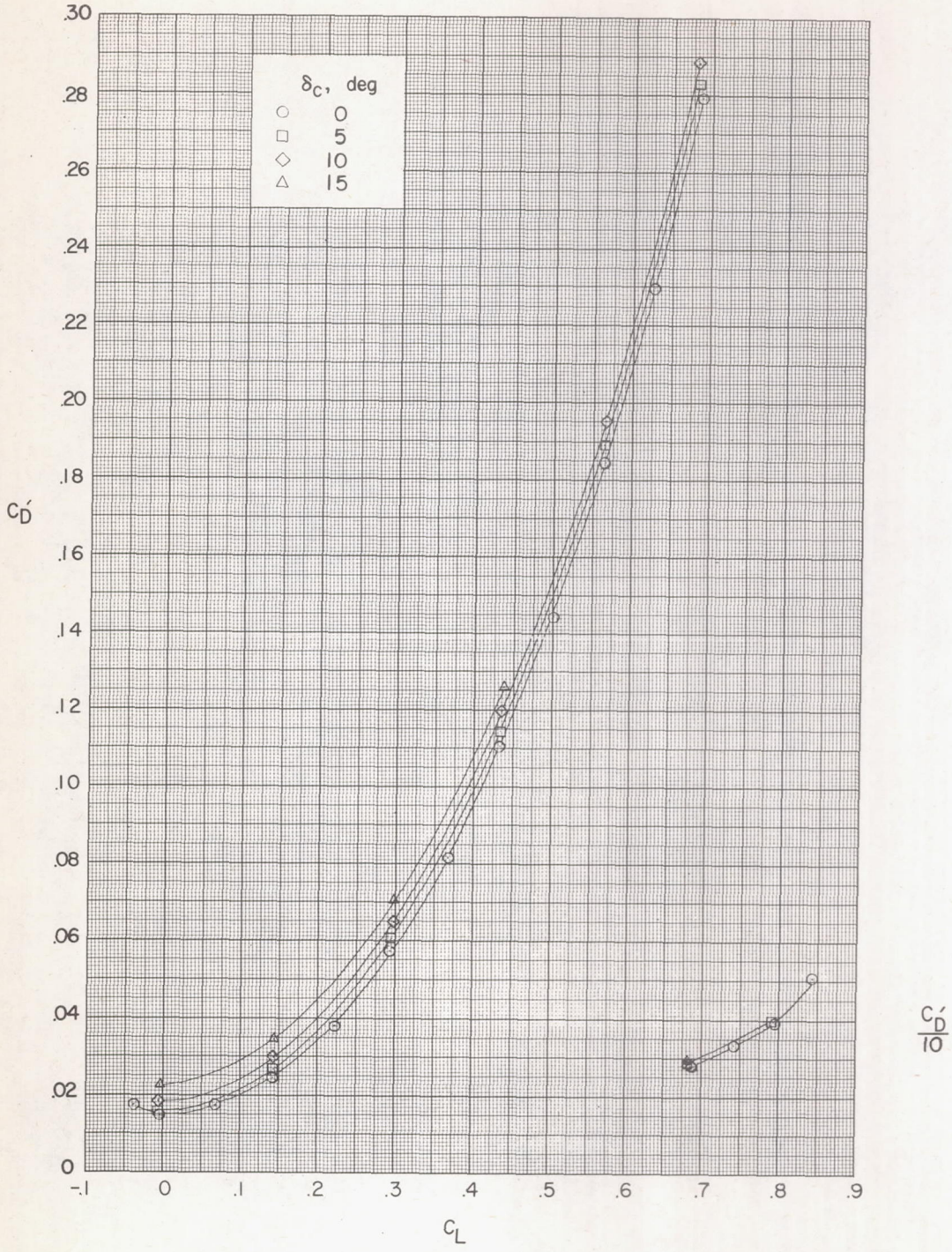
(c) Concluded.

Figure 6.- Concluded.



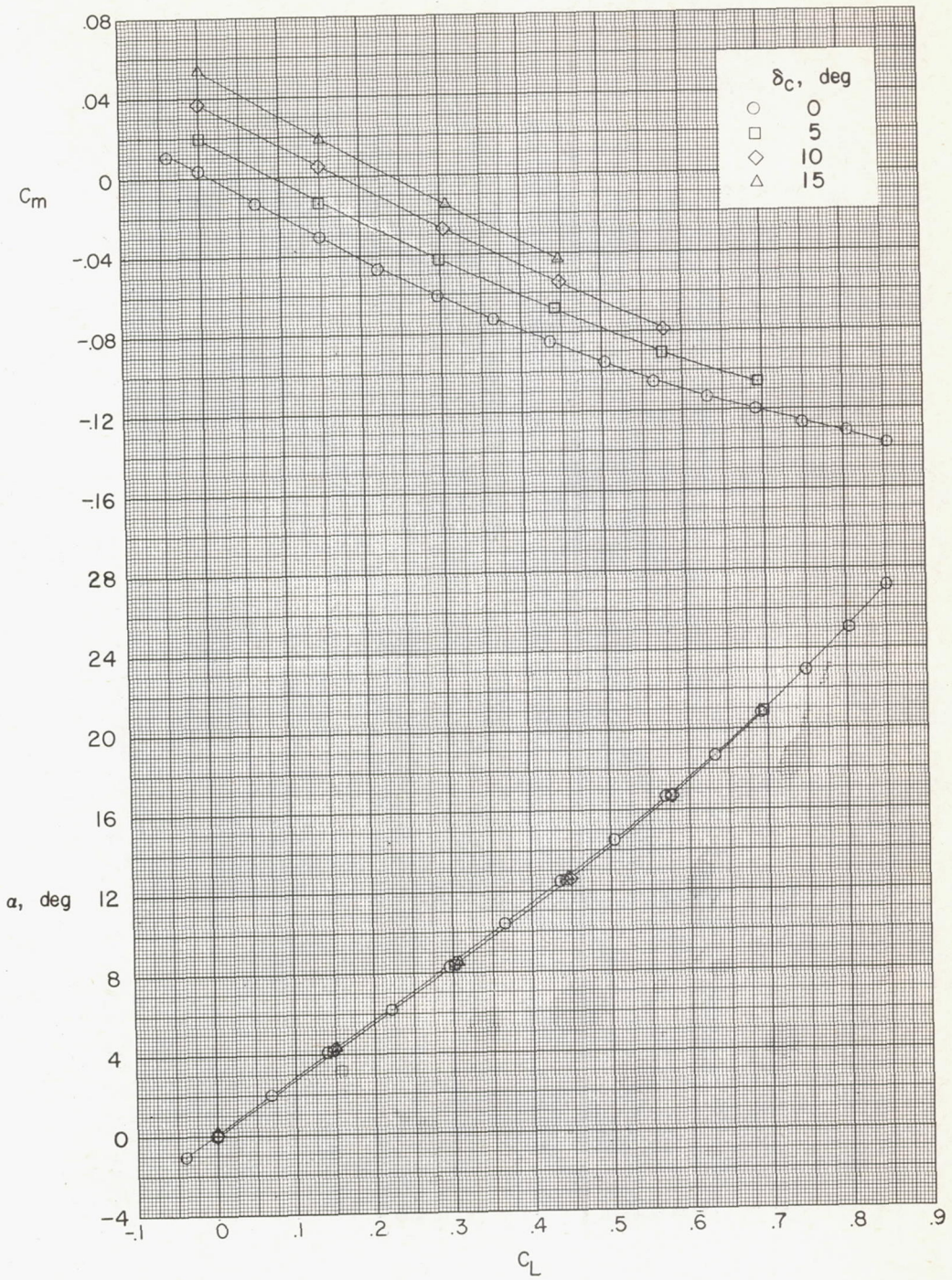
(a) $S_c/S_w = 0.051$.

Figure 7.- The aerodynamic characteristics in pitch of the configuration with the delta wing. M = 2.01.



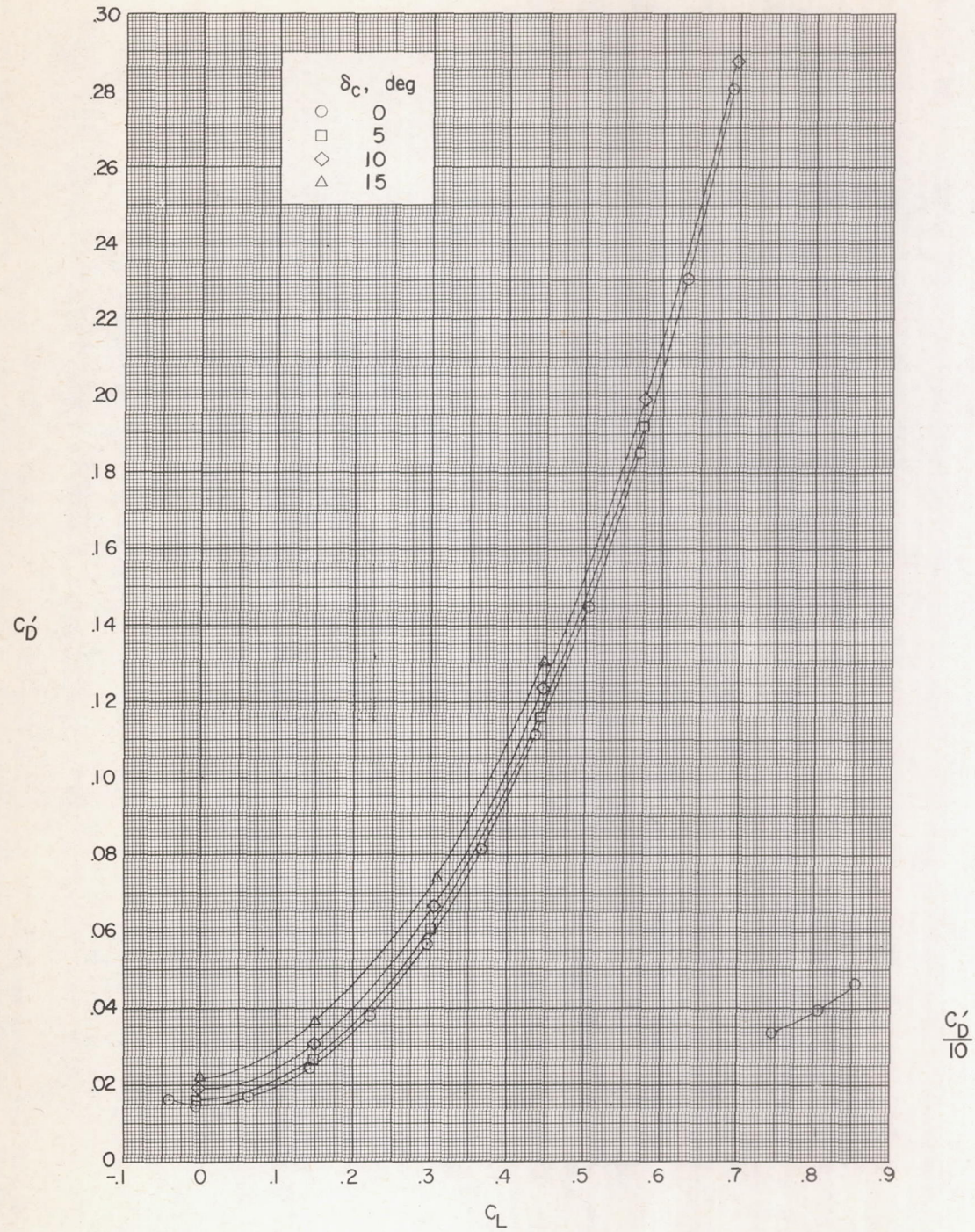
(a) Concluded.

Figure 7.- Continued.



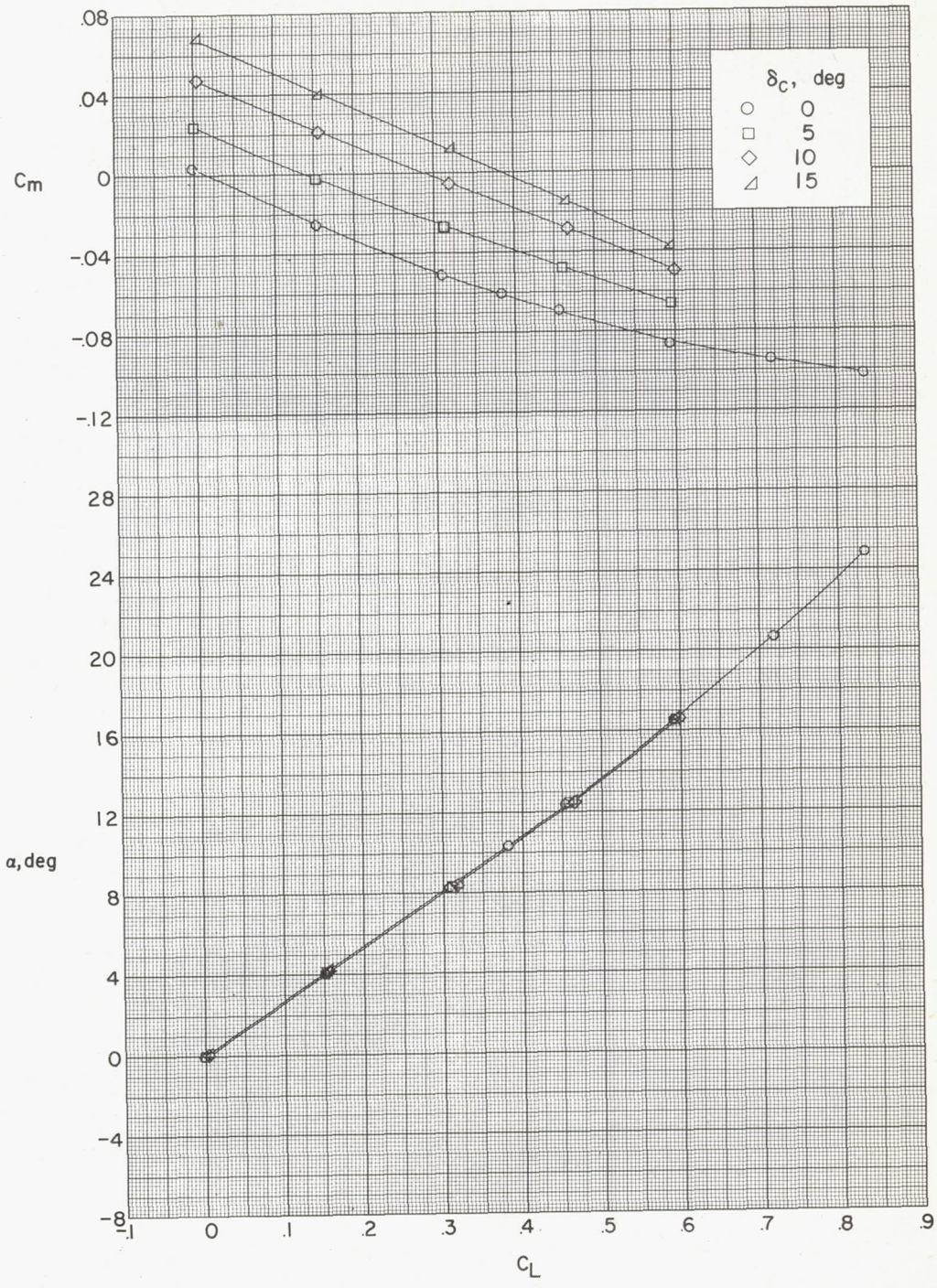
(b) $S_c/S_w = 0.062$.

Figure 7.- Continued.



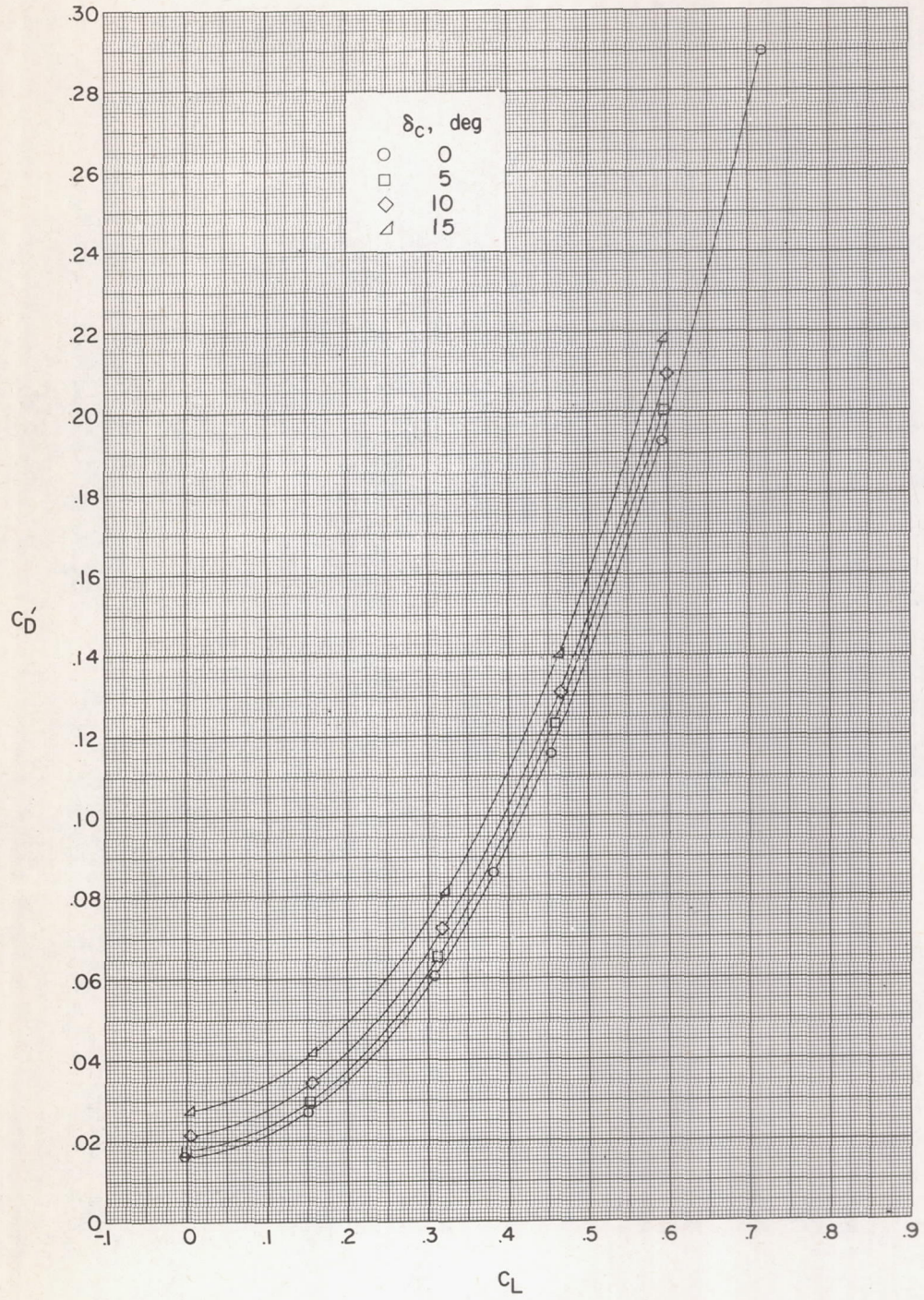
(b) Concluded.

Figure 7.- Continued.



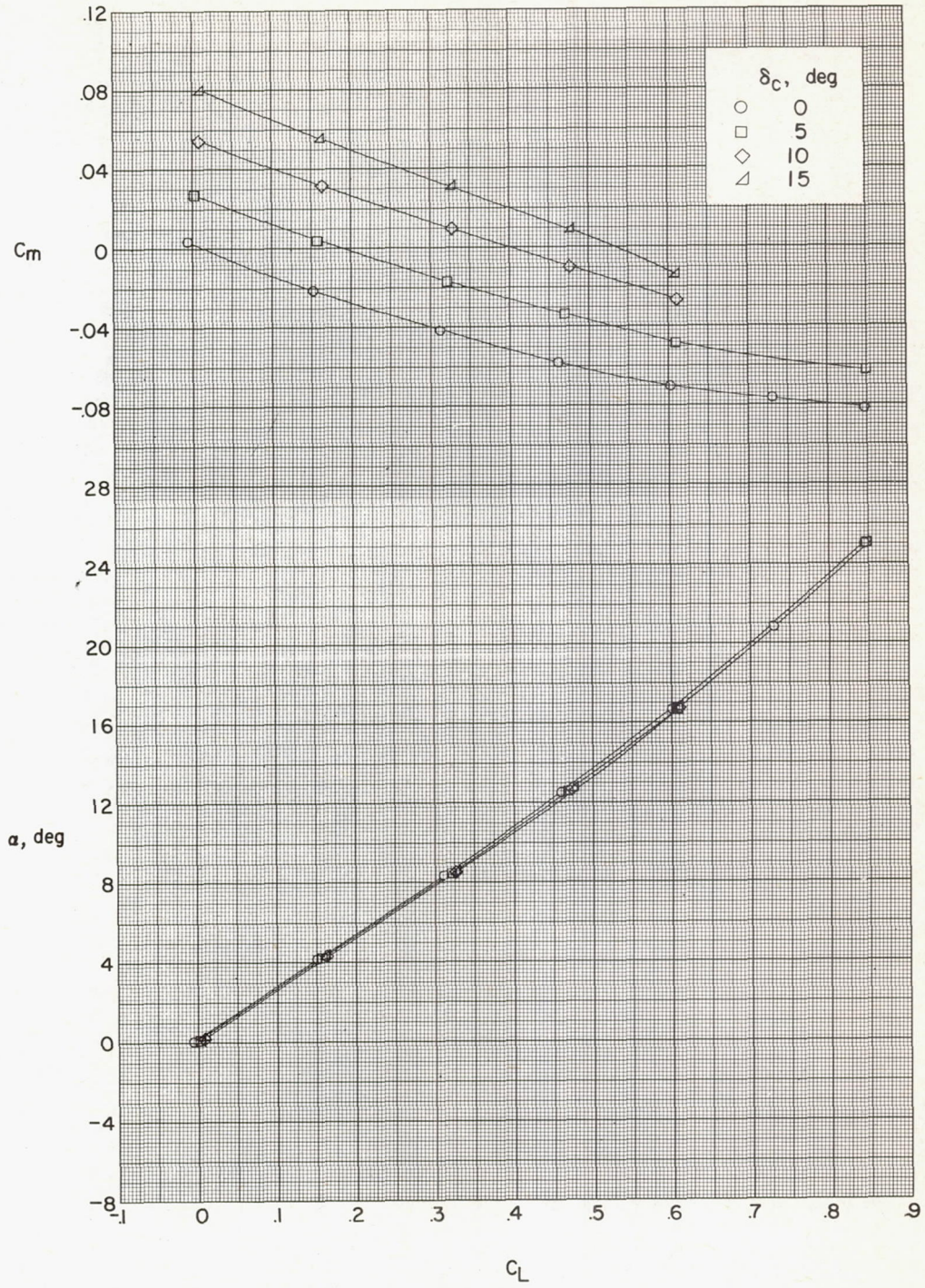
(c) $S_c/S_w = 0.082$.

Figure 7.- Continued.



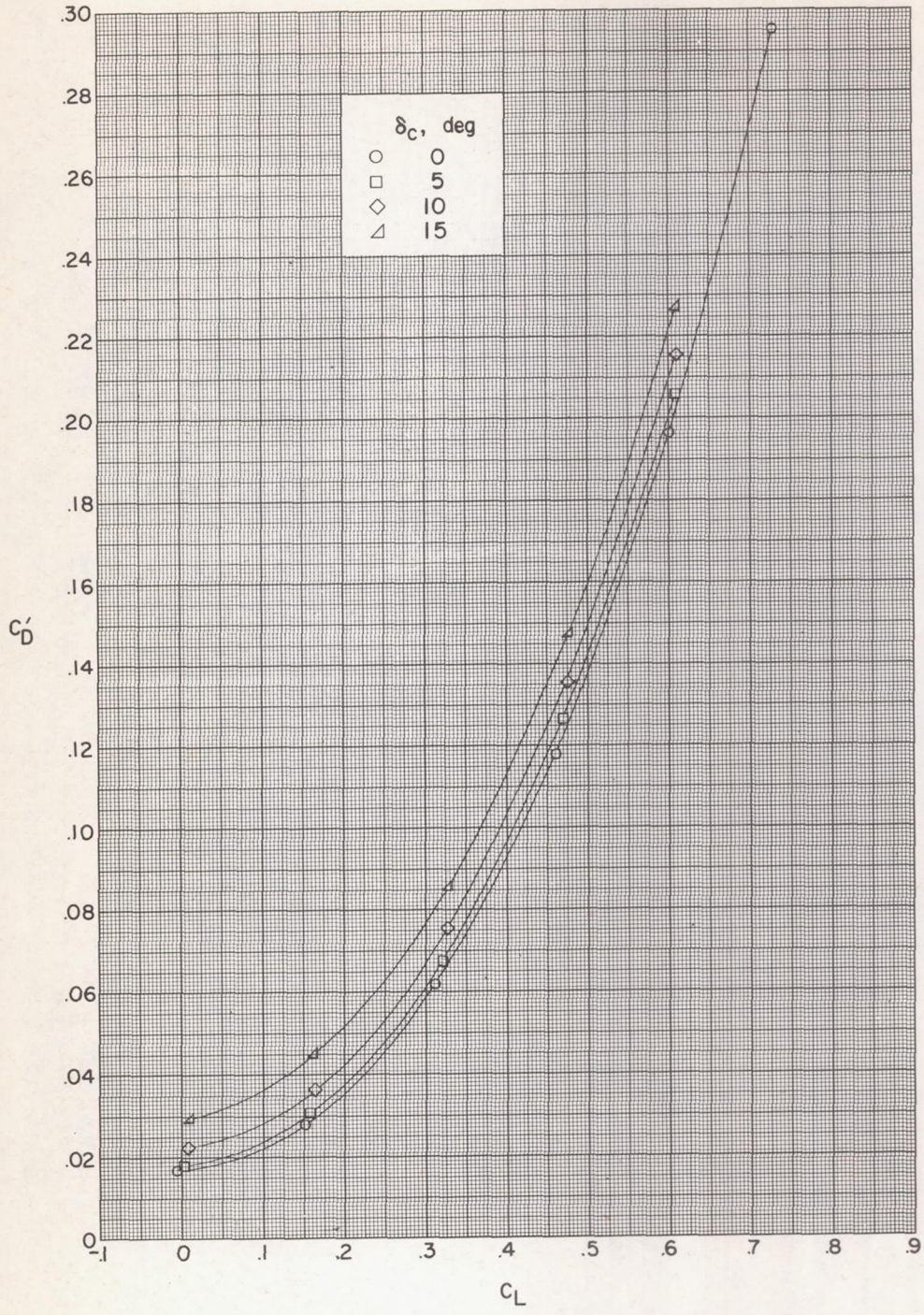
(c) Concluded.

Figure 7.- Continued.



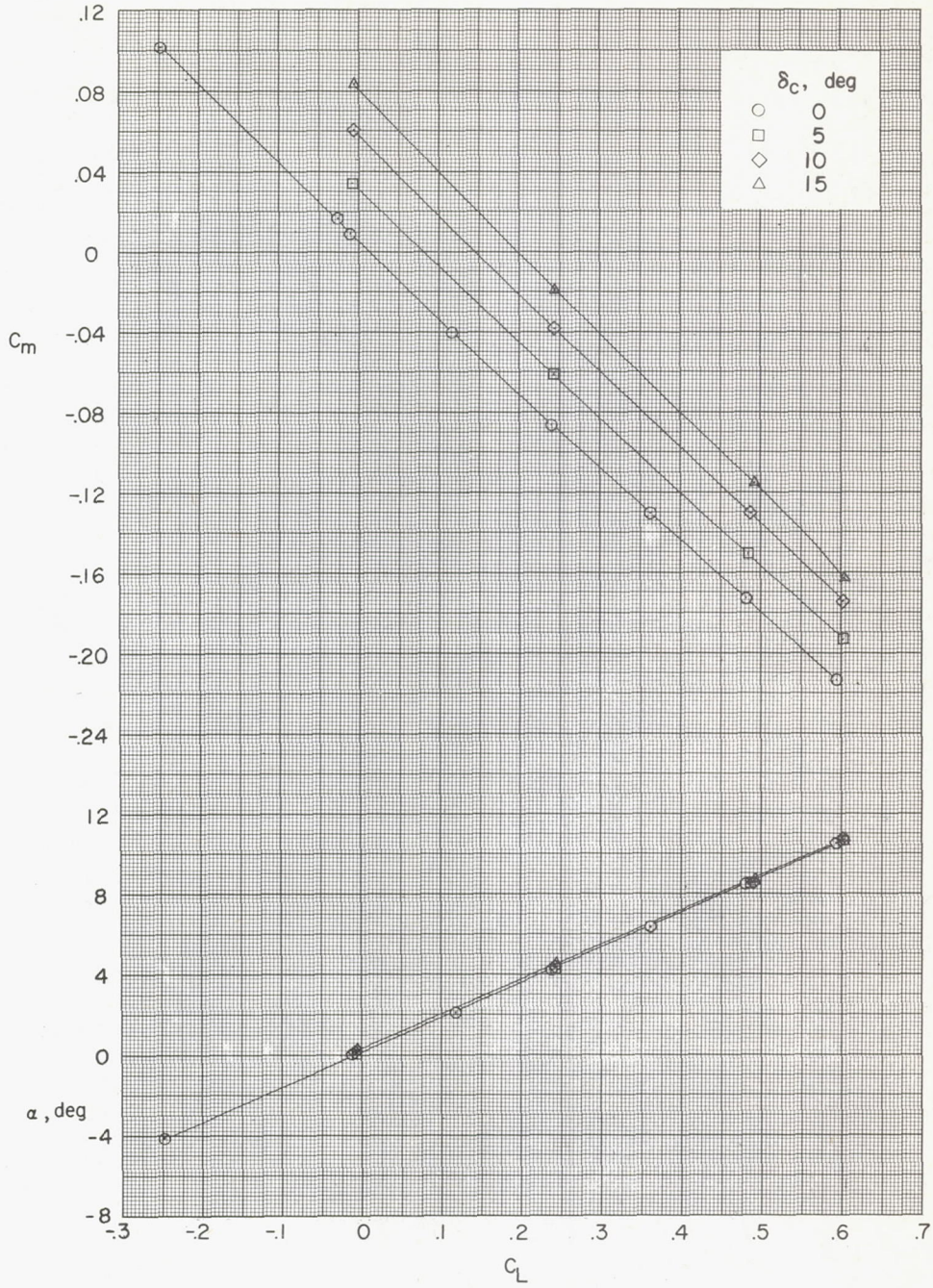
(d) $S_c/S_w = 0.096$.

Figure 7.- Continued.



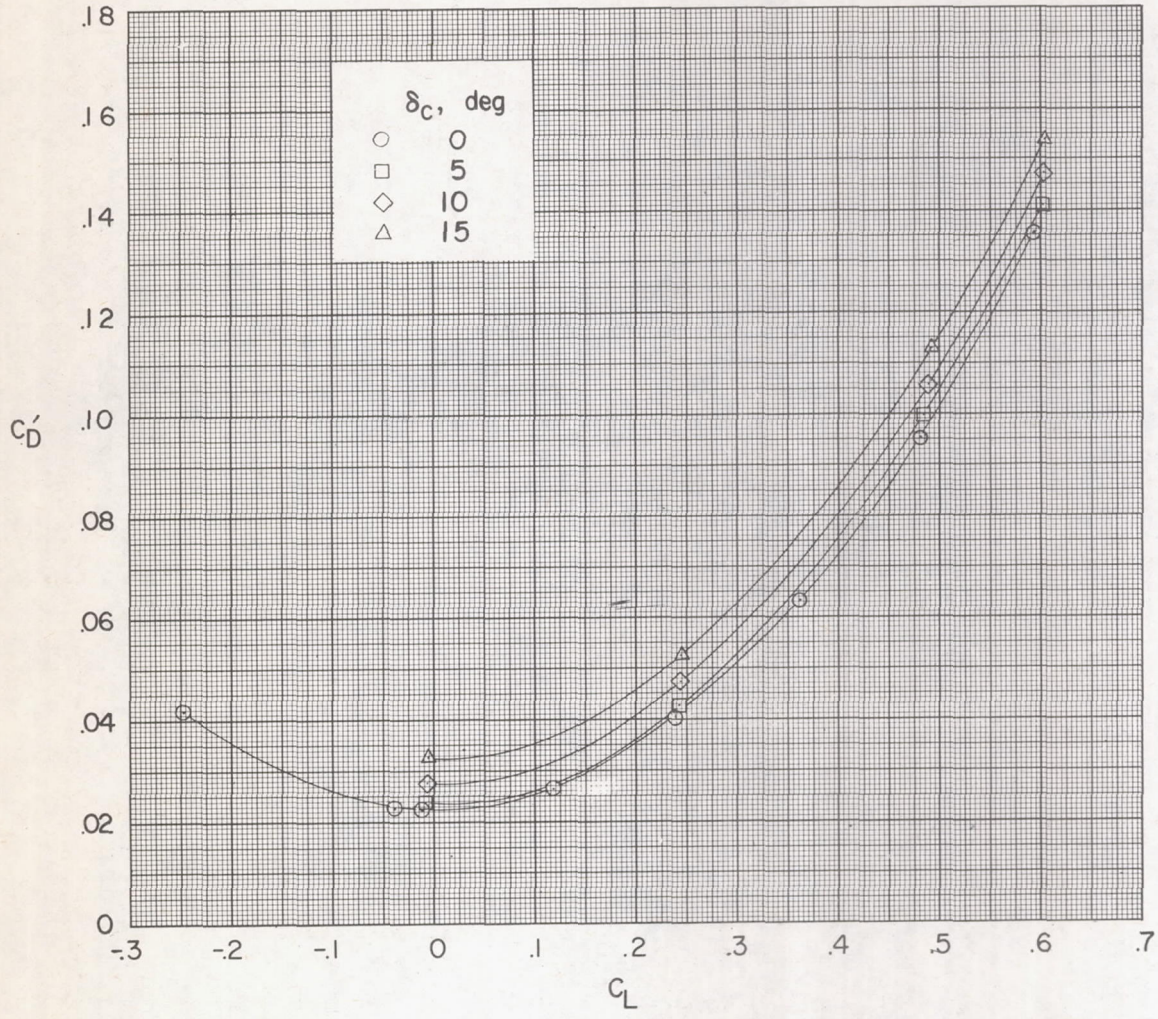
(d) Concluded.

Figure 7.- Concluded.



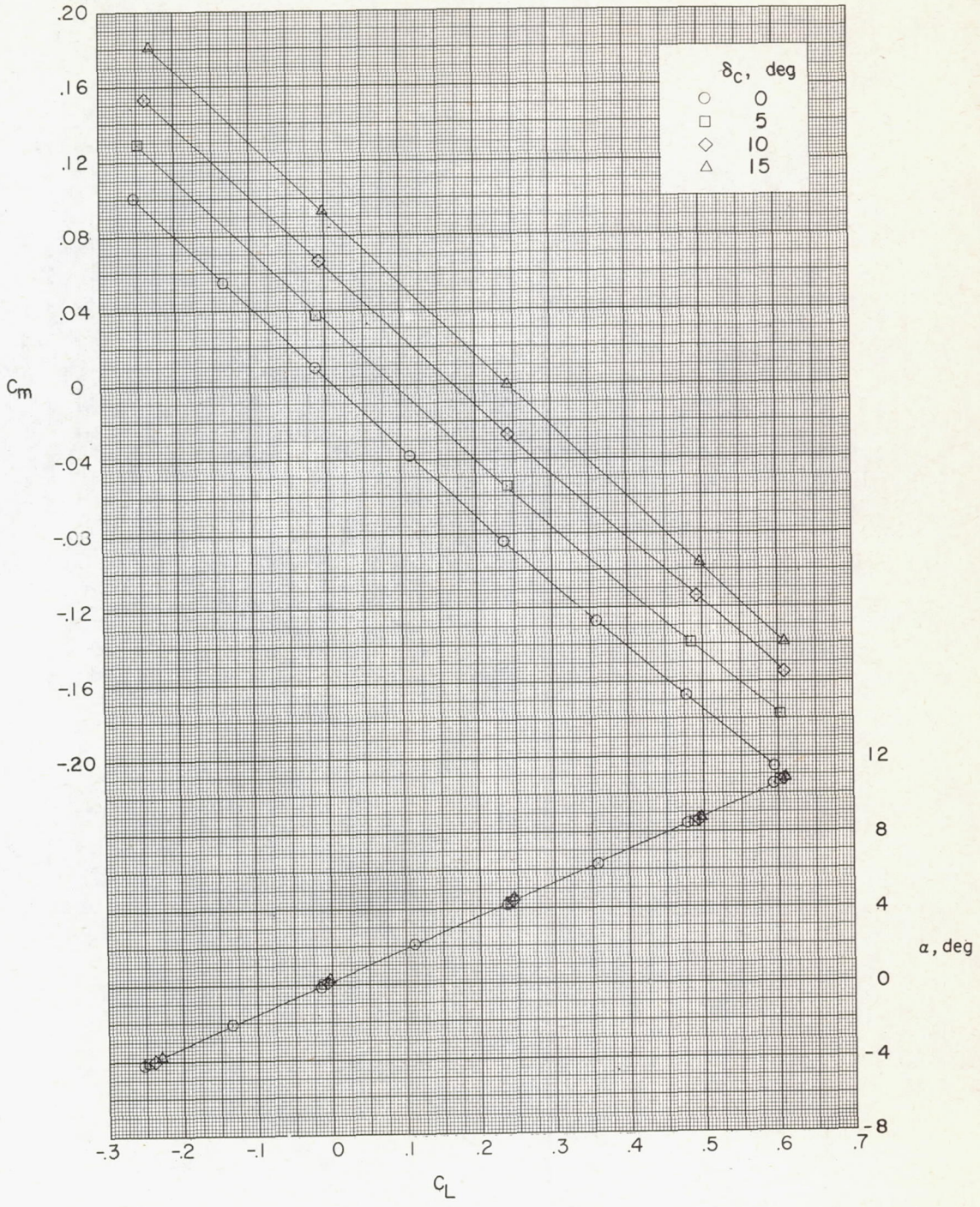
(a) $S_c/S_w = 0.051$.

Figure 8.- The aerodynamic characteristics in pitch of the configuration with the trapezoidal wing. M = 1.41.



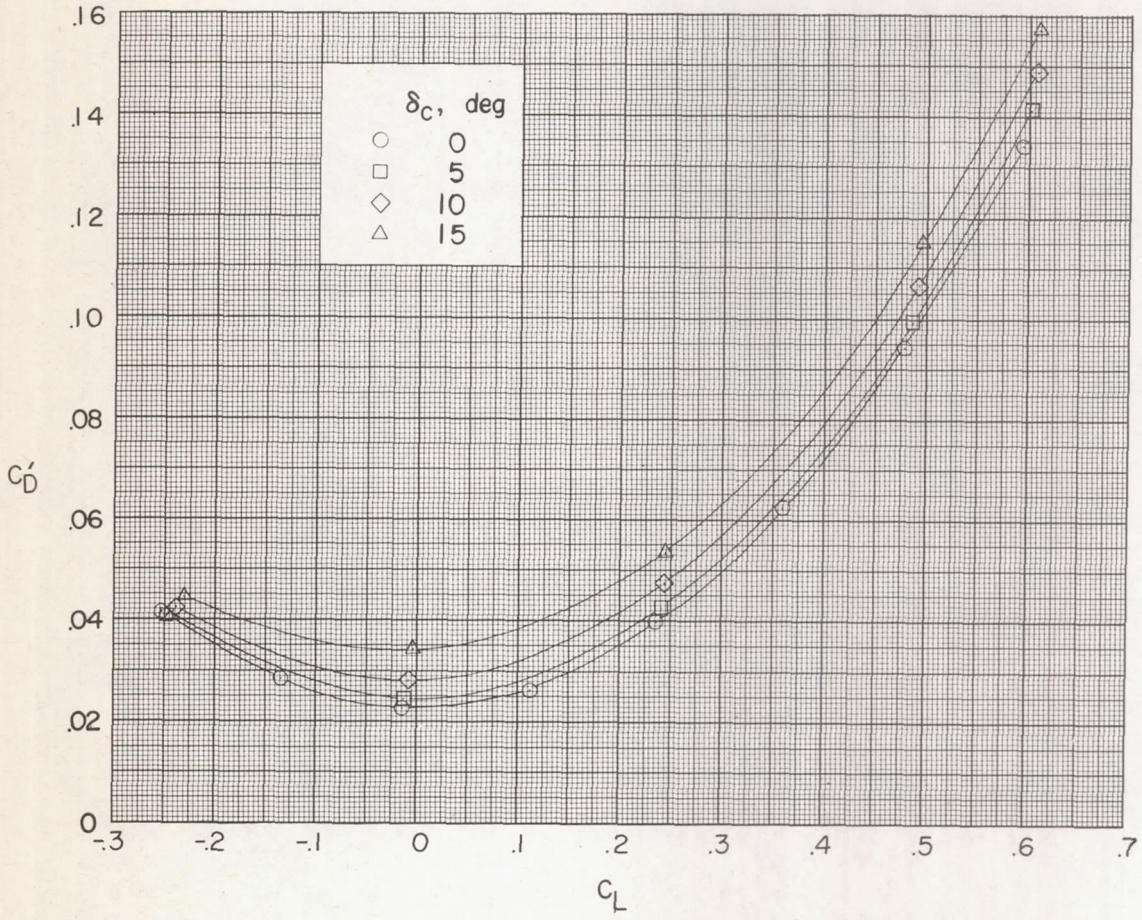
(a) Concluded.

Figure 8.- Continued.



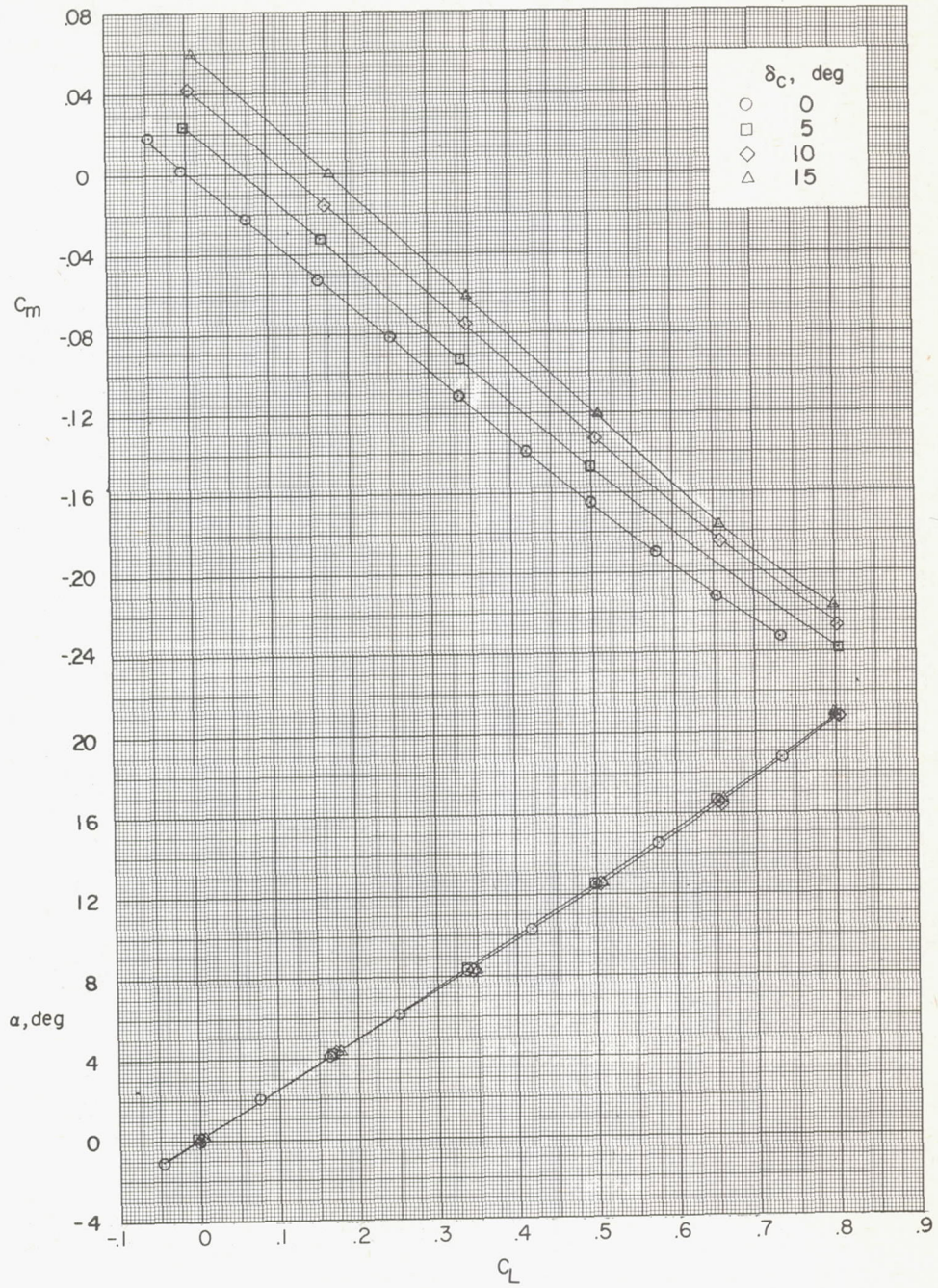
(b) $S_c/S_w = 0.062$.

Figure 8.- Continued.



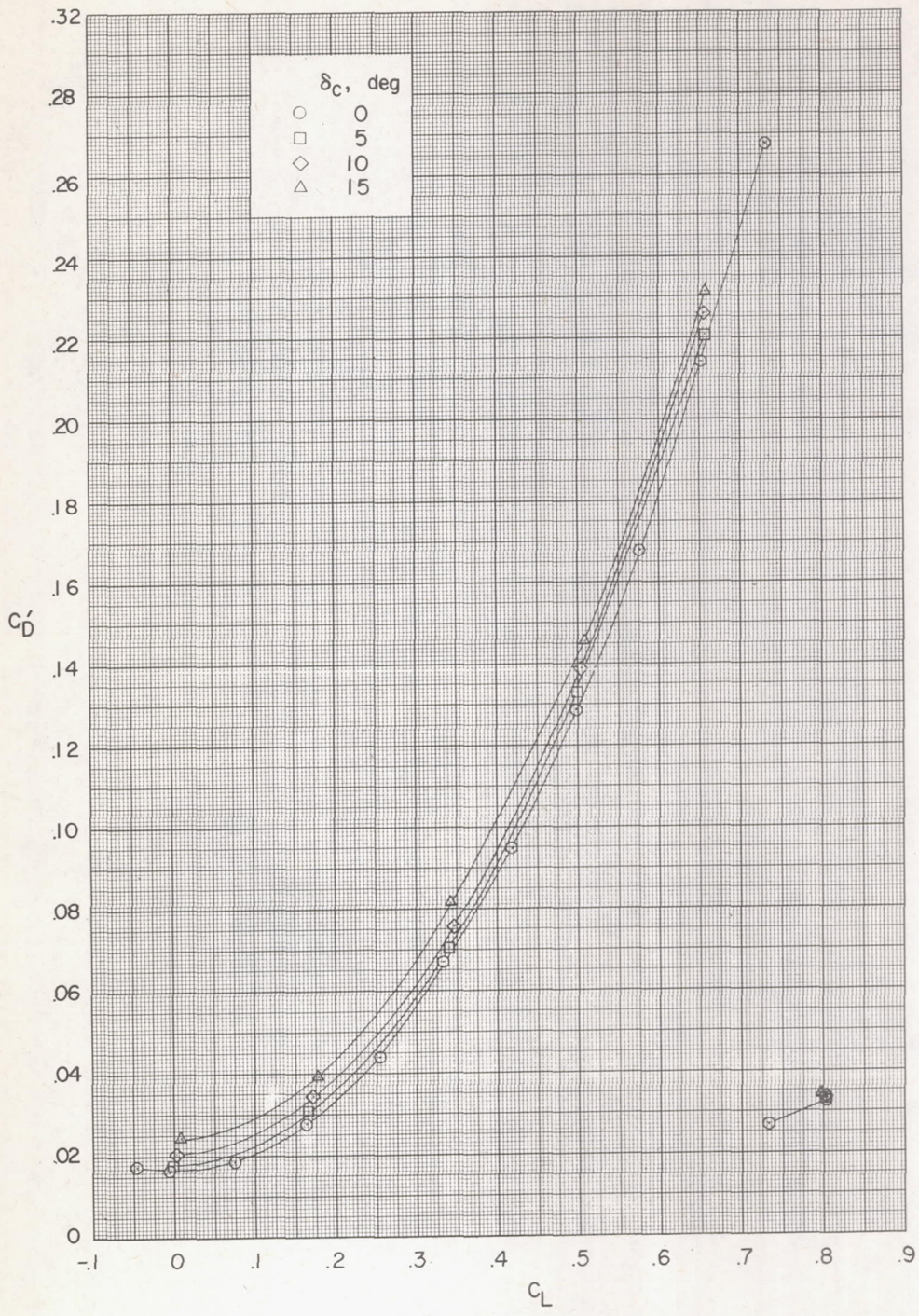
(b) Concluded.

Figure 8.- Concluded.



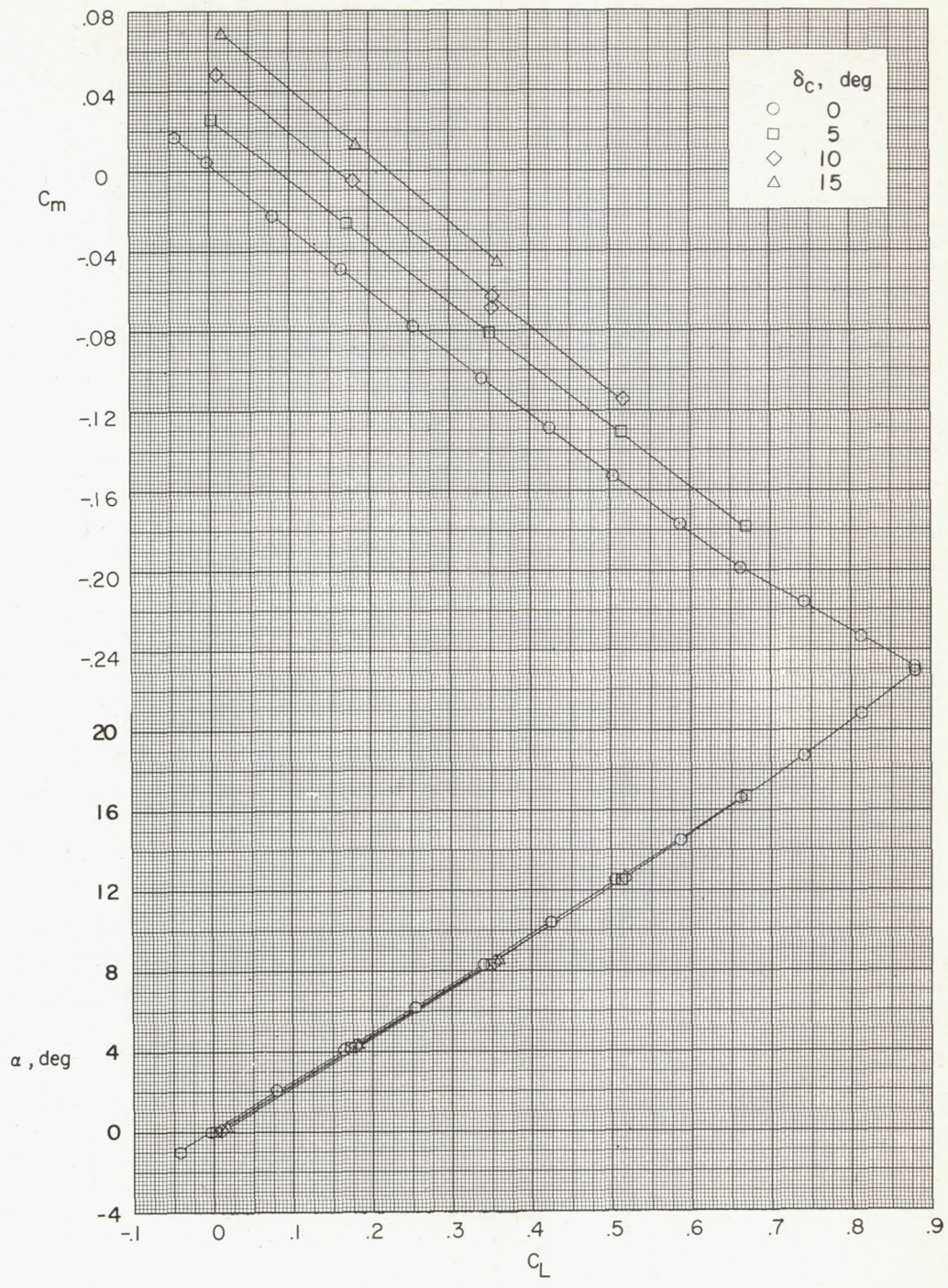
(a) $S_c/S_w = 0.051$.

Figure 9.- The aerodynamic characteristics in pitch of the configuration with the trapezoidal wing. M = 2.01.



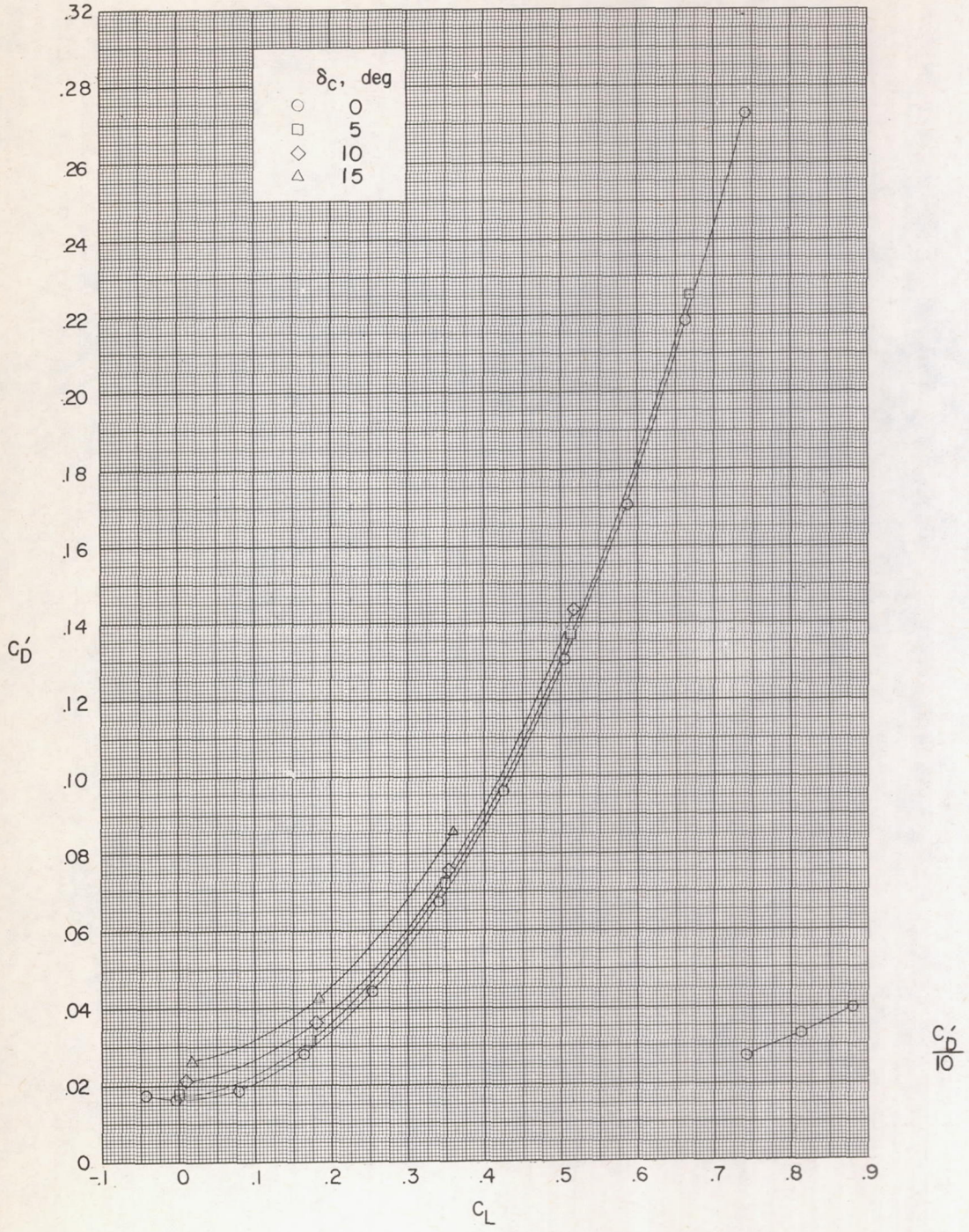
(a) Concluded.

Figure 9.- Continued.



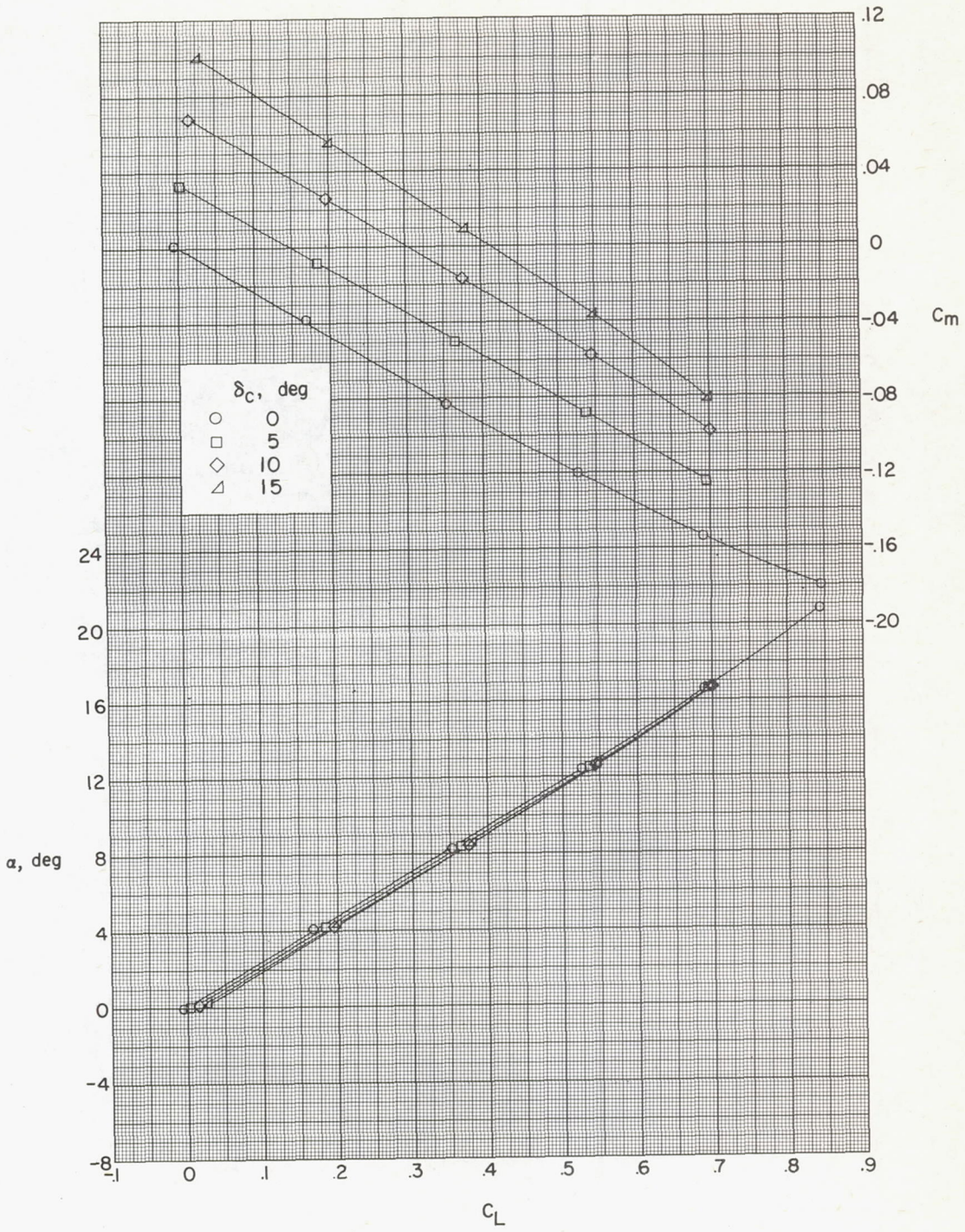
(b) $S_c/S_w = 0.062$.

Figure 9.- Continued.



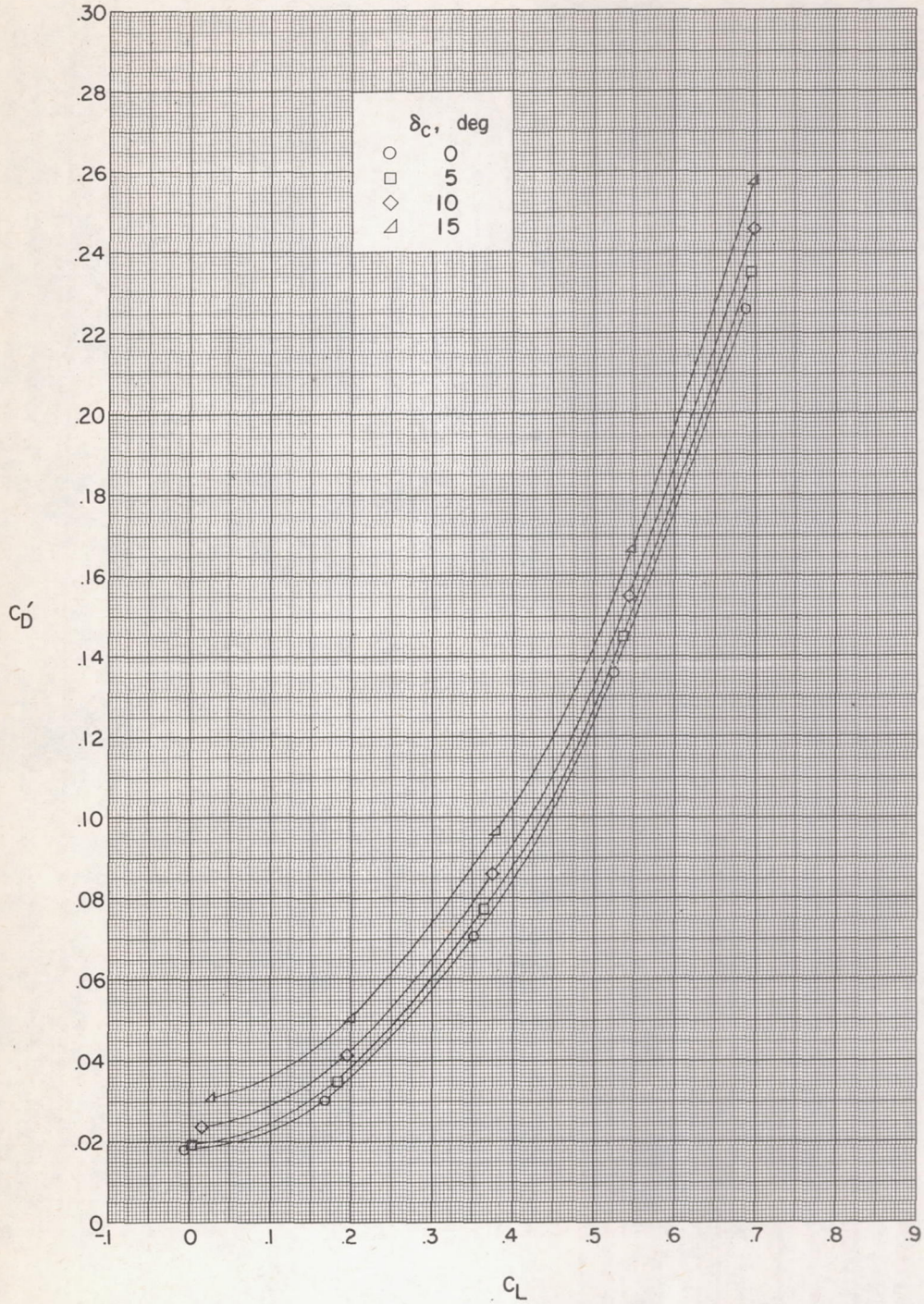
(b) Concluded.

Figure 9.- Continued.



(c) $S_c/S_w = 0.096$.

Figure 9.- Continued.



(c) Concluded.

Figure 9.- Concluded.

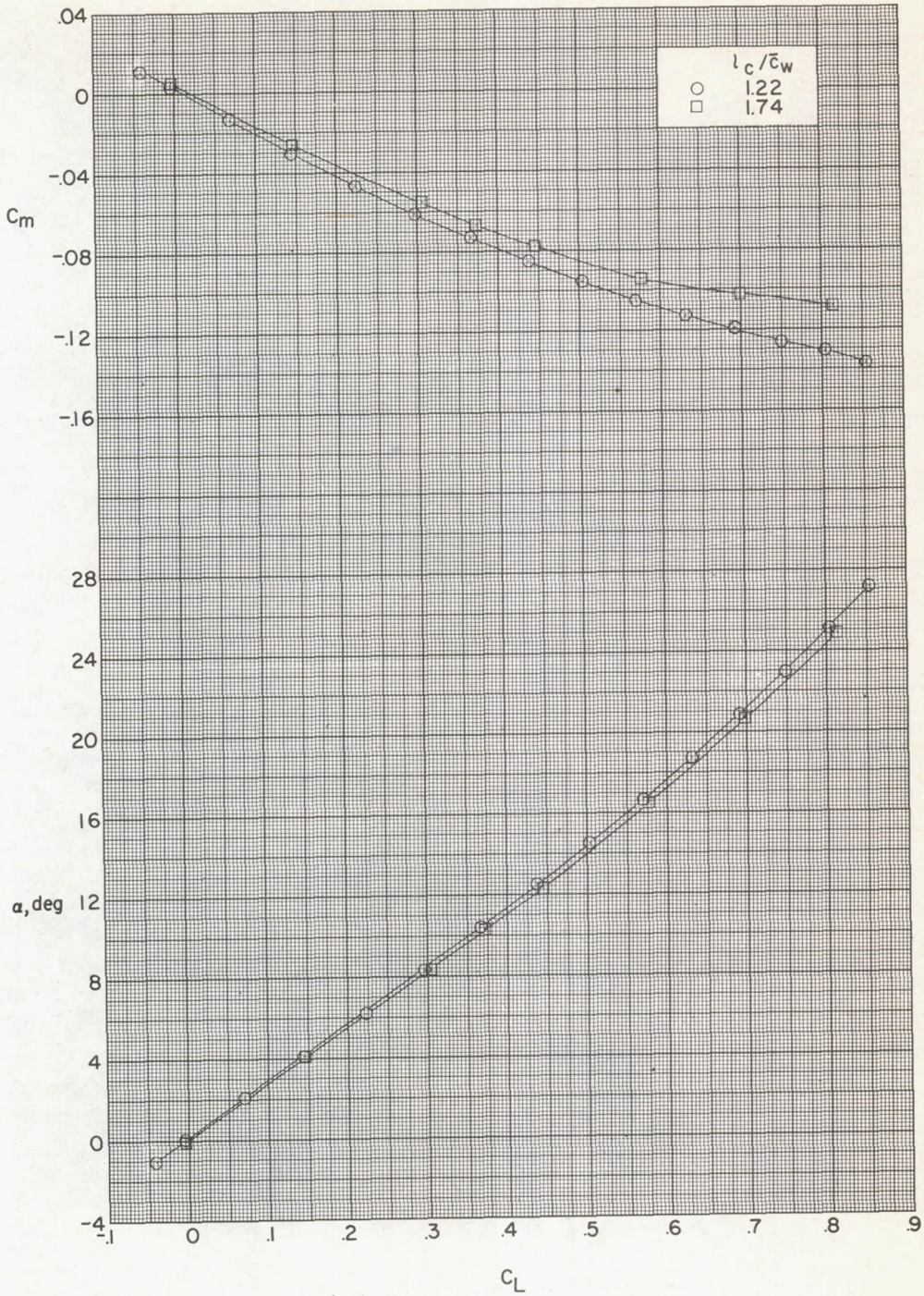


Figure 10.- Effect of canard moment arm on aerodynamic characteristics in pitch. Delta wing; S_c/S_w = 0.062; M = 2.01.

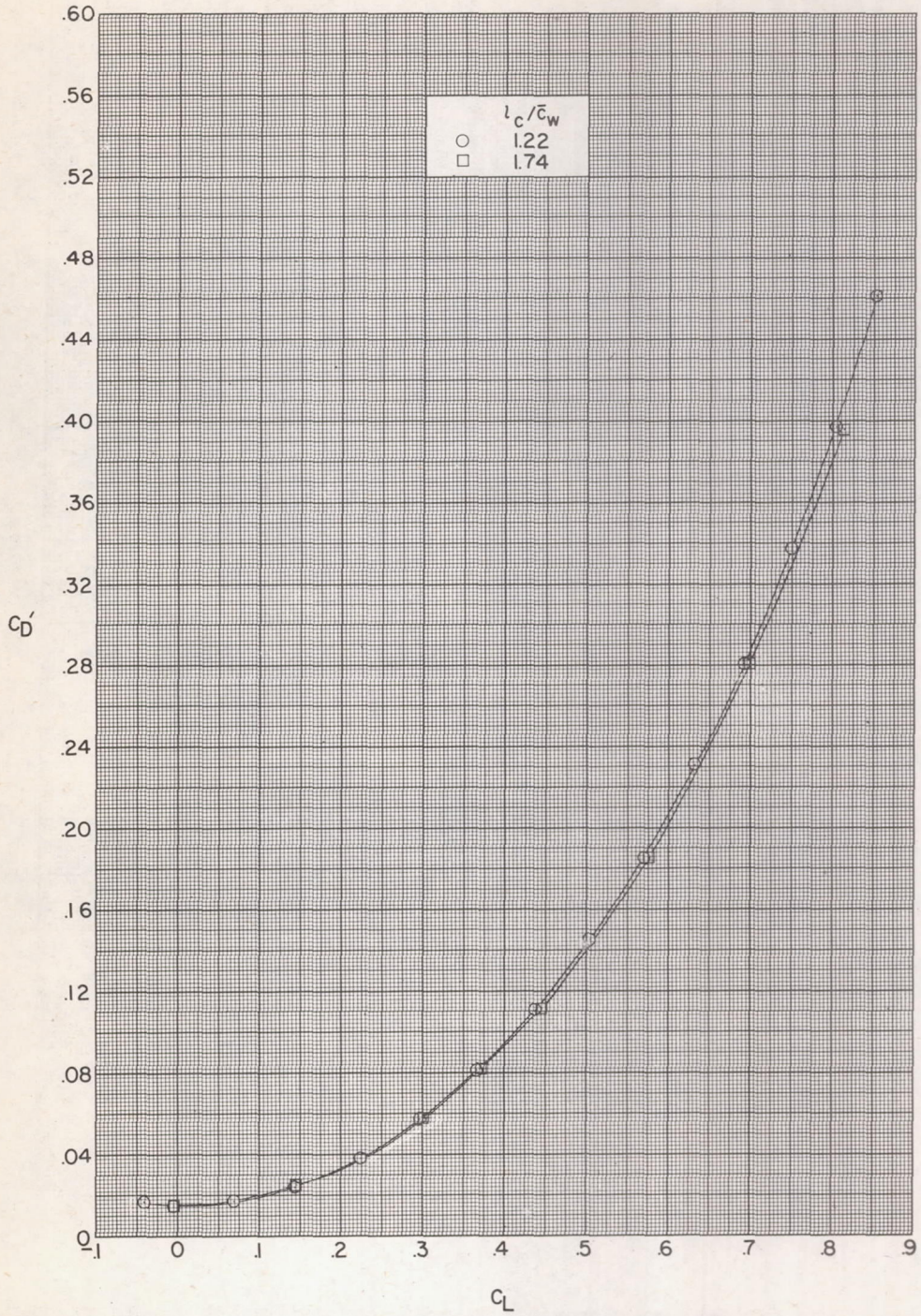
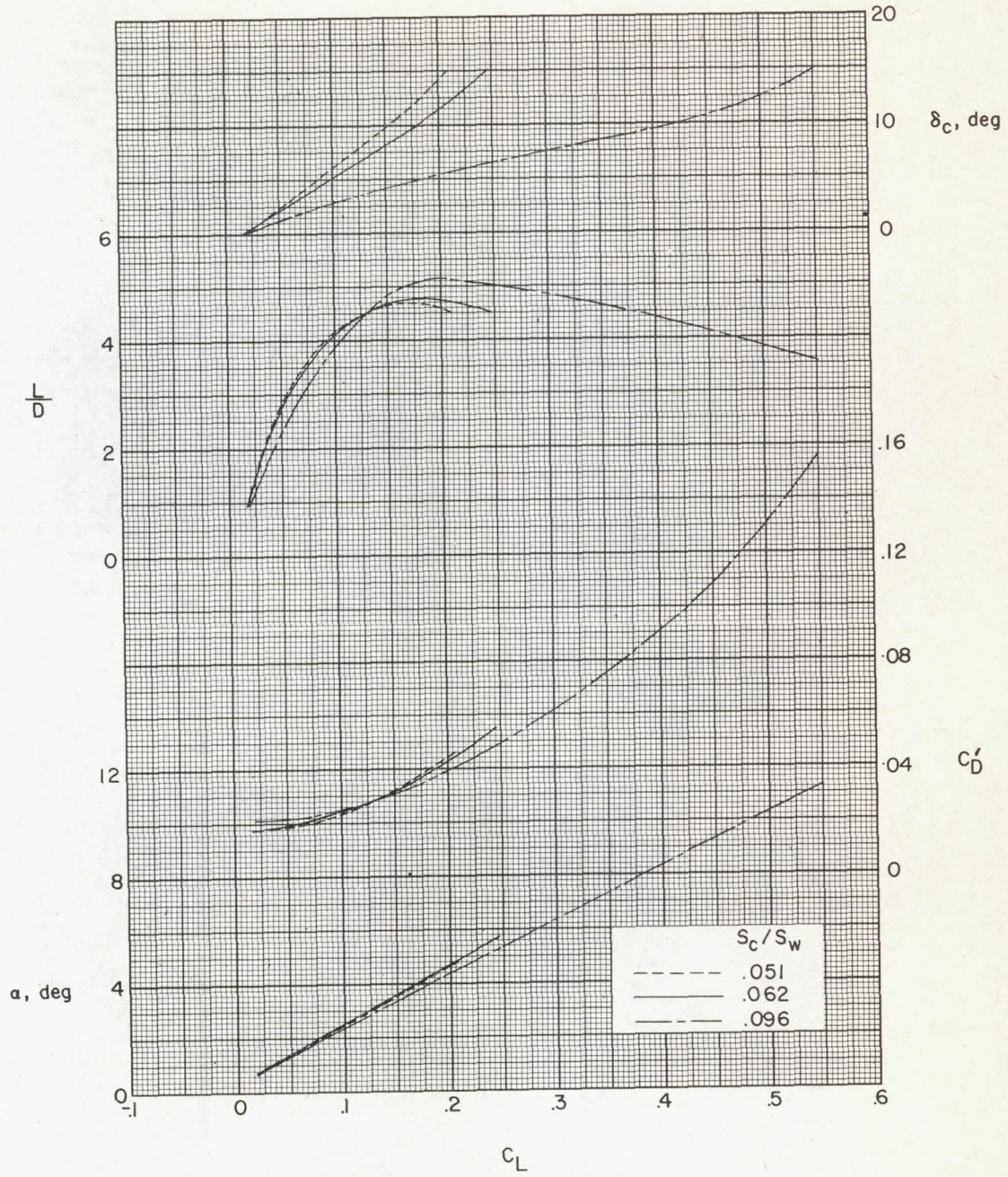
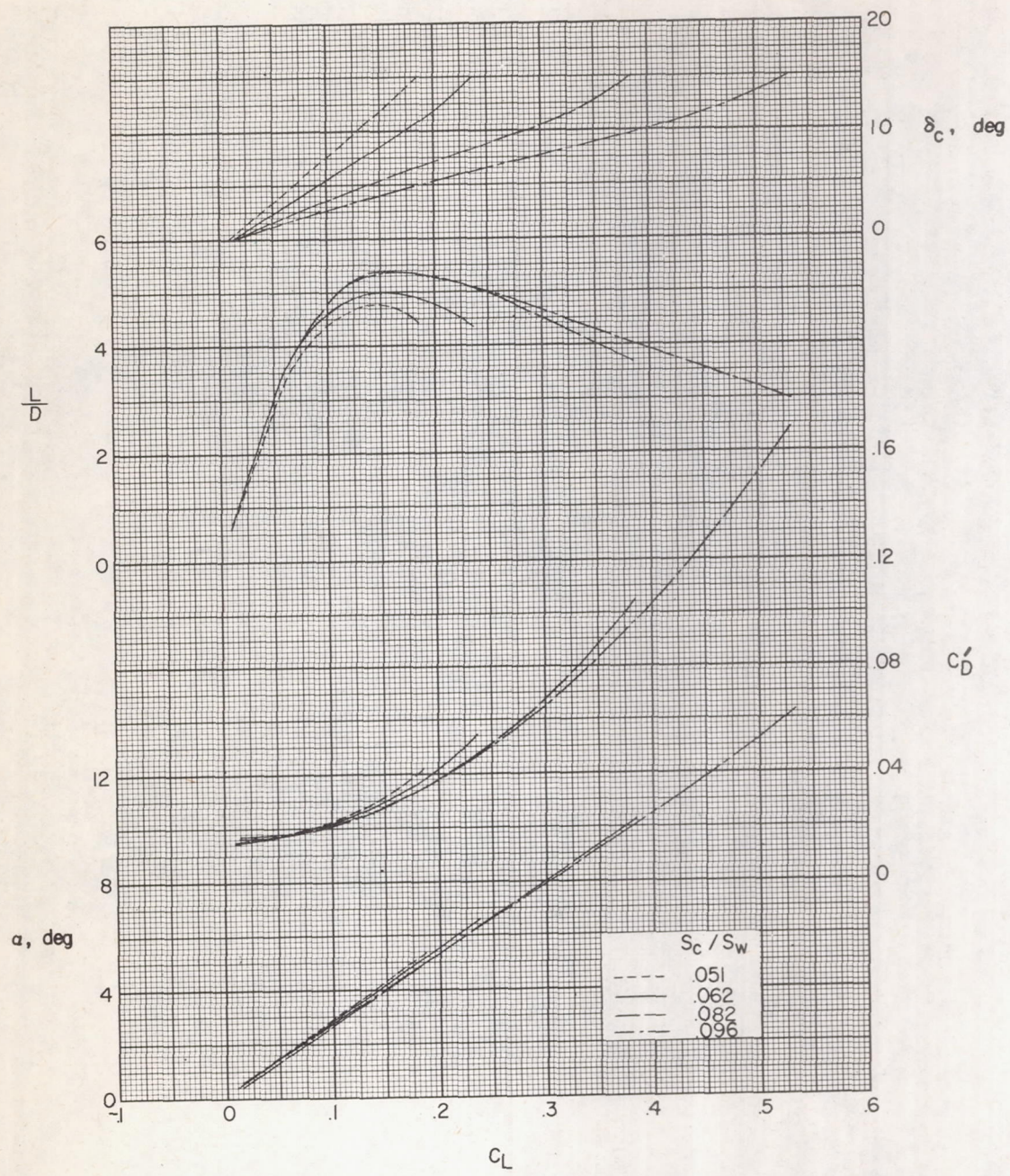


Figure 10.- Concluded.



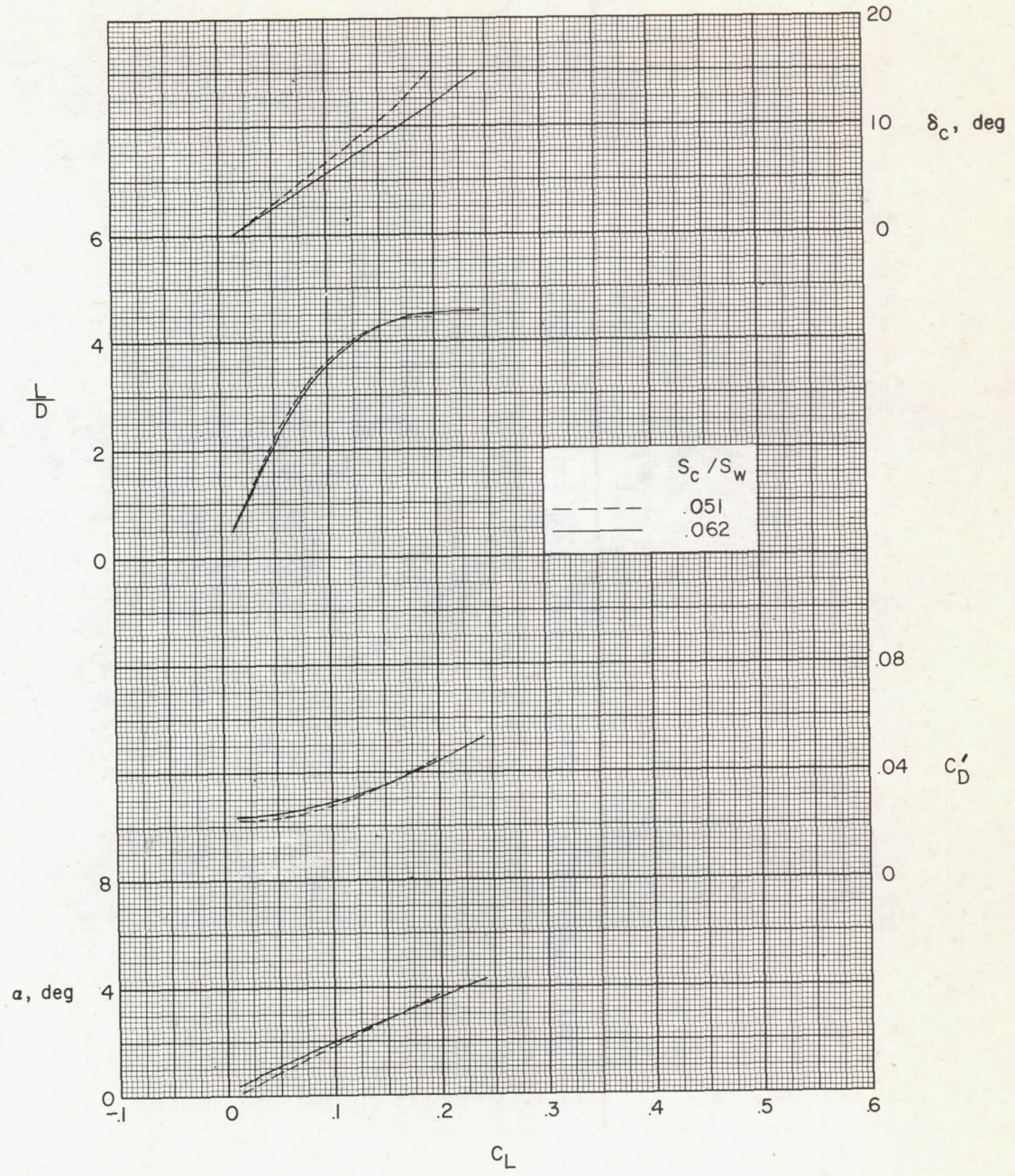
(a) M = 1.41.

Figure 11.- Effect of canard size on longitudinal trim characteristics. Delta wing; $l_c/\bar{c}_w$ = 1.22.



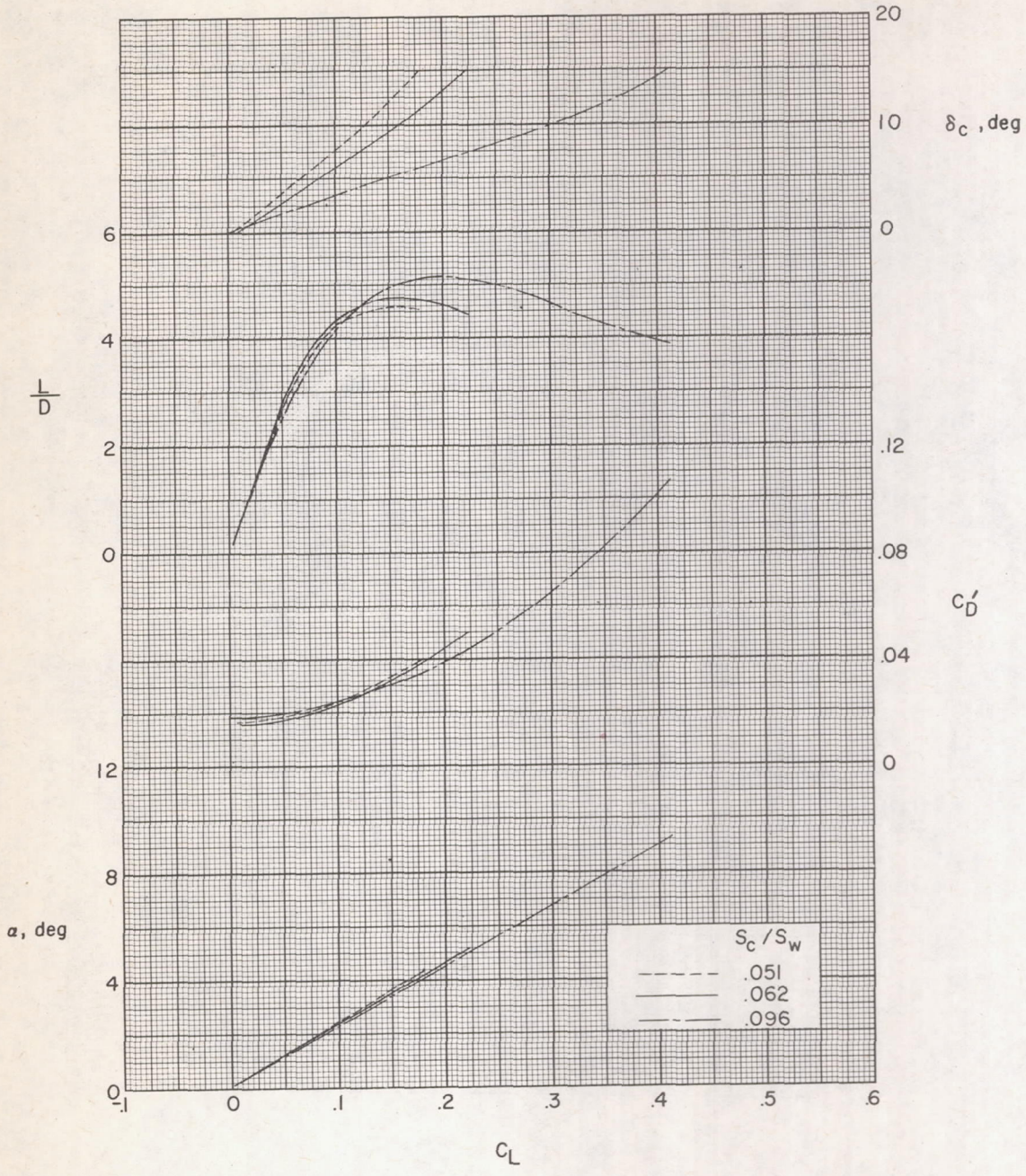
(b) M = 2.01.

Figure 11.- Concluded.



(a) M = 1.41.

Figure 12.- Effect of canard size on longitudinal trim characteristics. Trapezoidal wing; $l_c/\bar{c}_w = 1.22$.



(b) M = 2.01.

Figure 12.- Concluded.

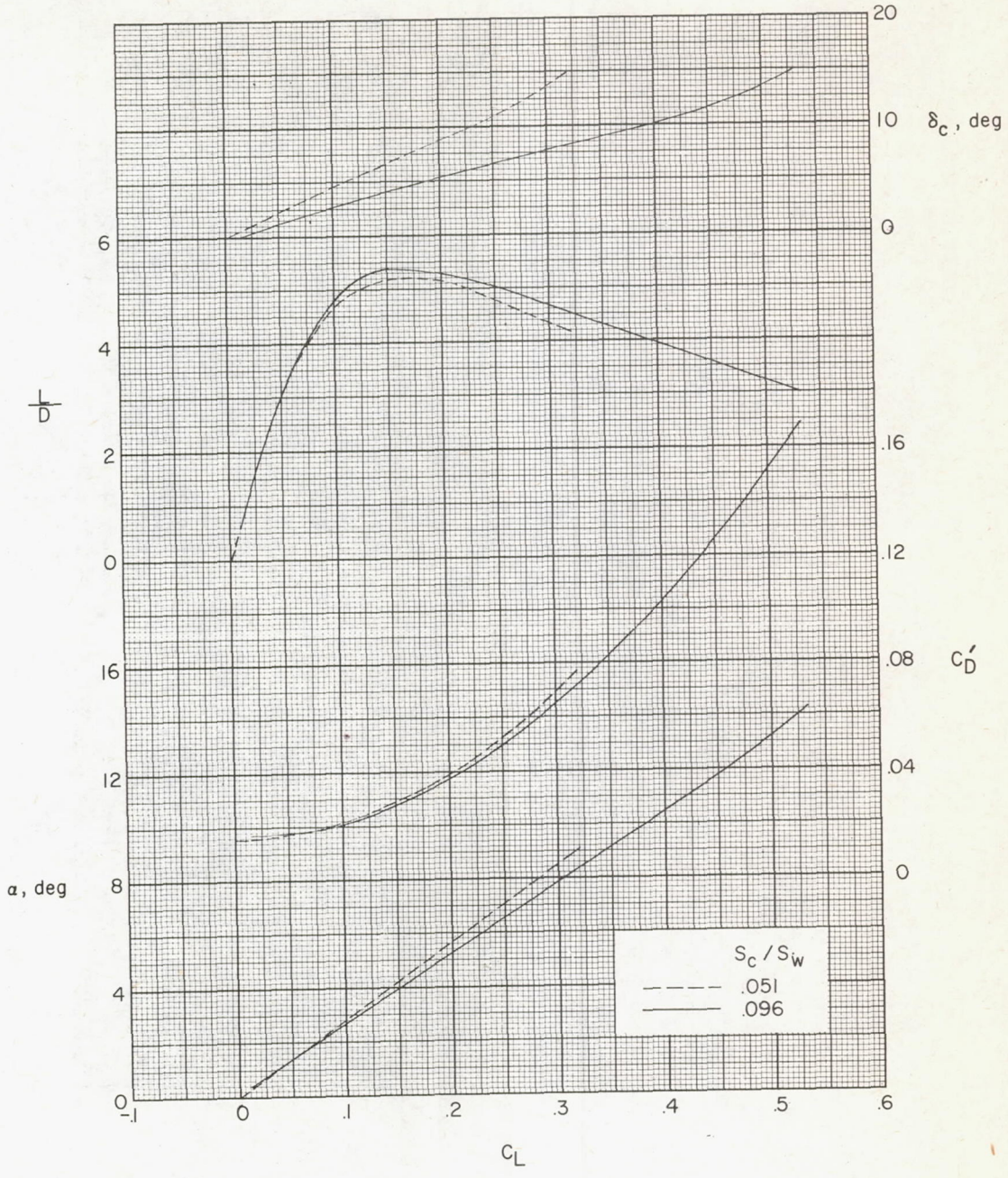
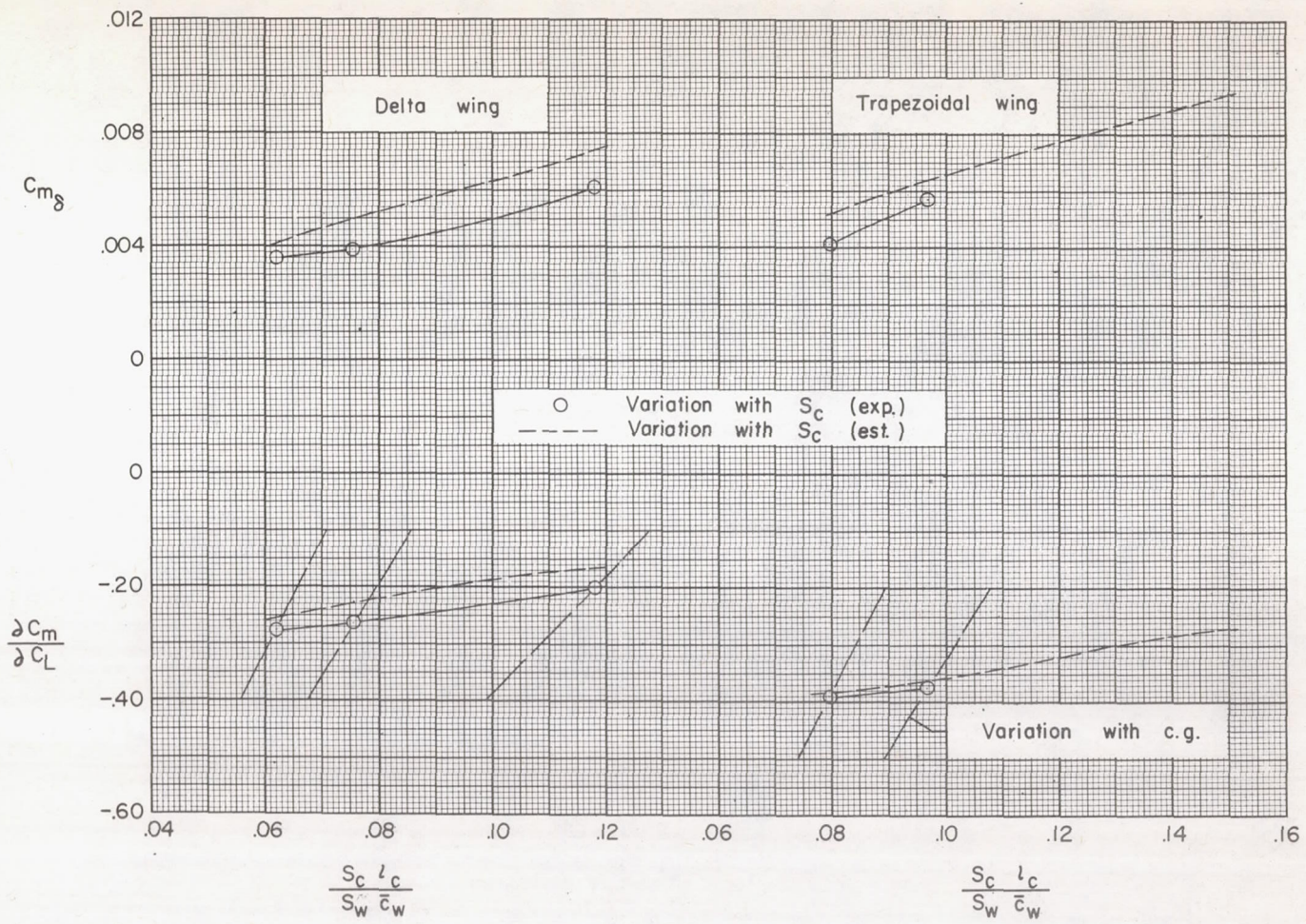
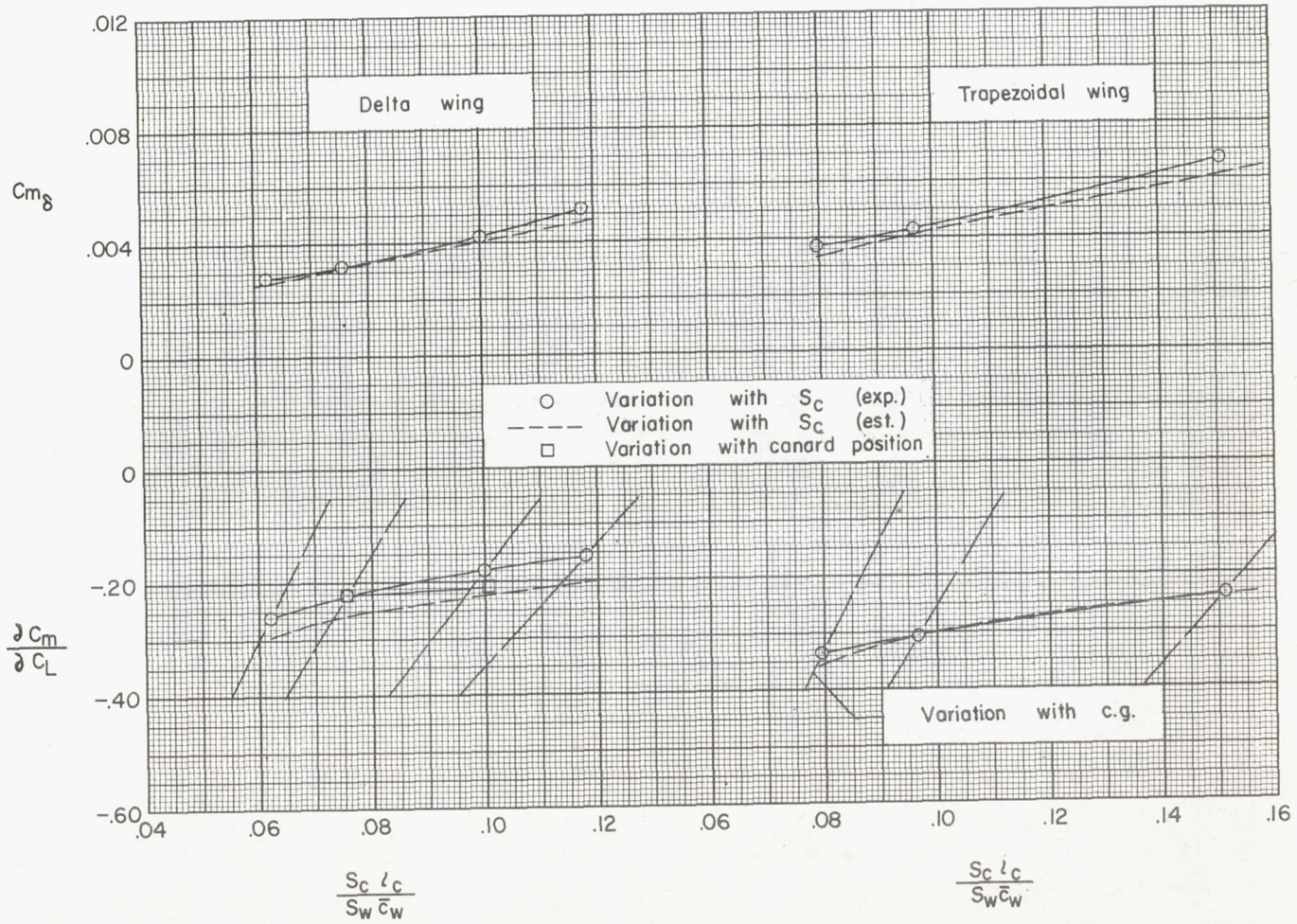


Figure 13.- Effect of canard size on longitudinal trim characteristics with constant static margin of 15.6 percent $\bar{c}_w$. Delta wing; M = 2.01.



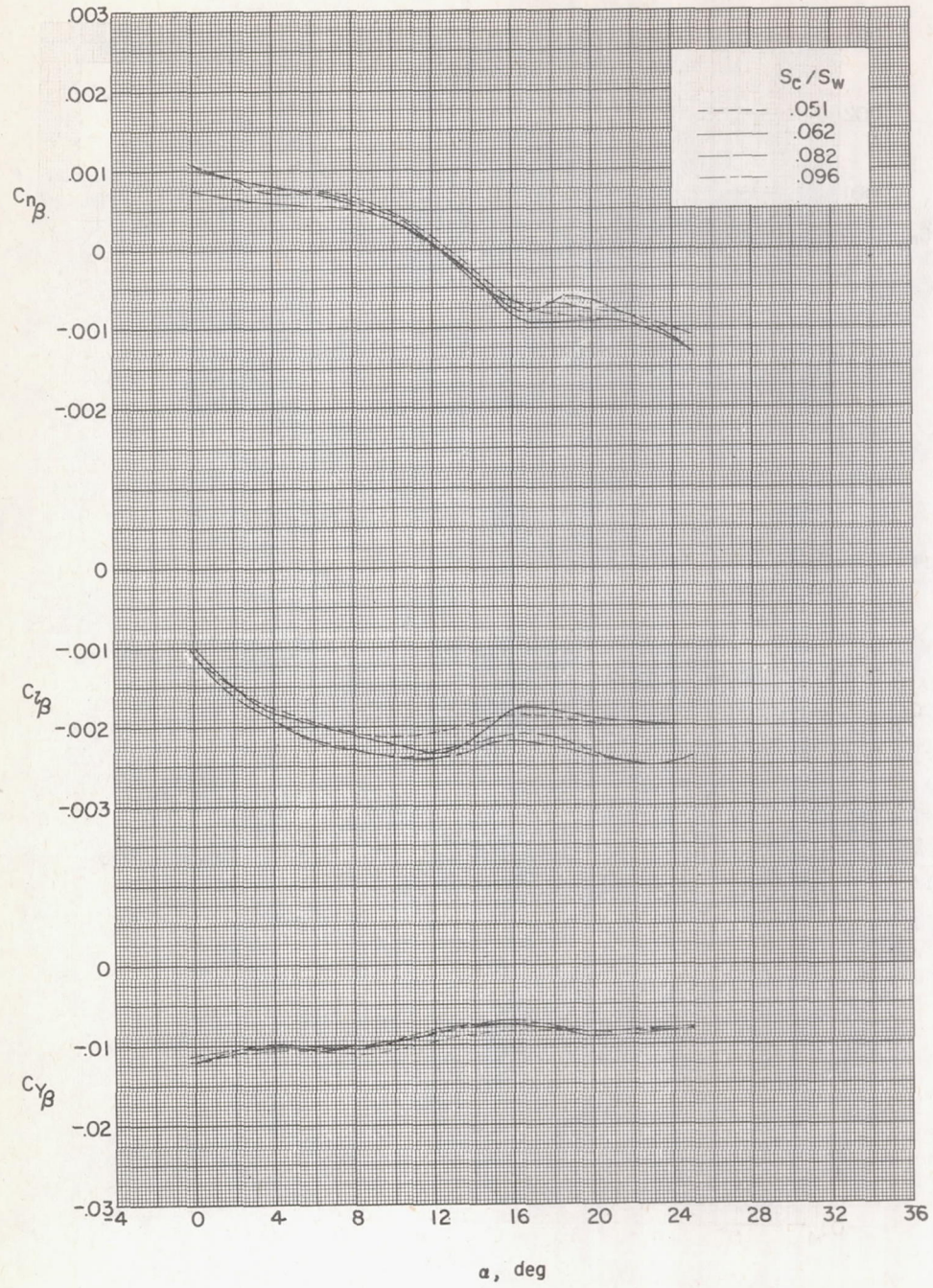
(a) M = 1.41.

Figure 14.- Variation of longitudinal stability and control parameters with canard volume coefficient. $C_L \approx 0$.



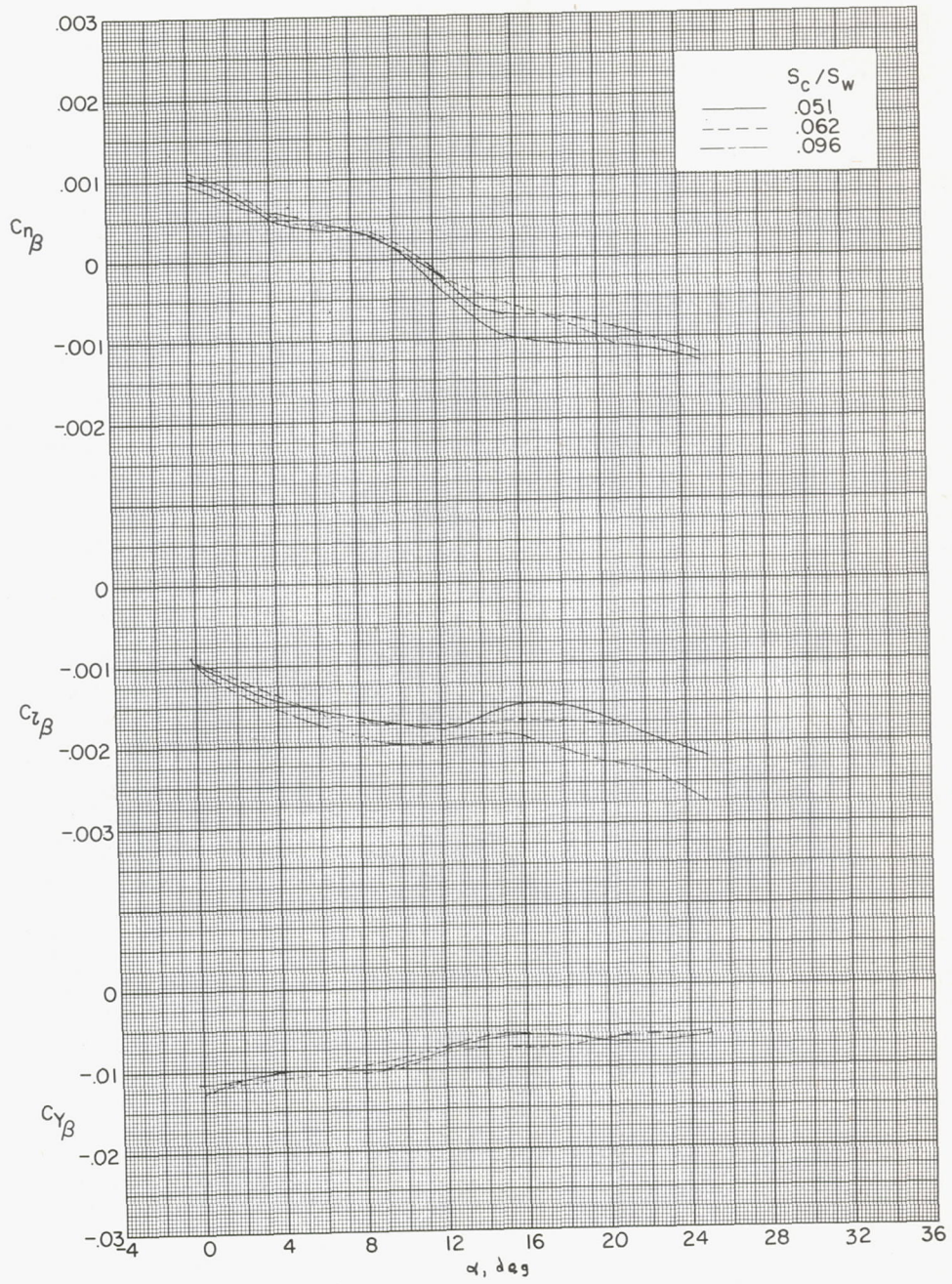
(b) M = 2.01.

Figure 14.- Concluded.



(a) Delta wing.

Figure 15.- Effect of canard size on sideslip characteristics. $l_c/\bar{c}_w$ = 1.22; M = 2.01.



(b) Trapezoidal wing.

Figure 15.- Concluded.

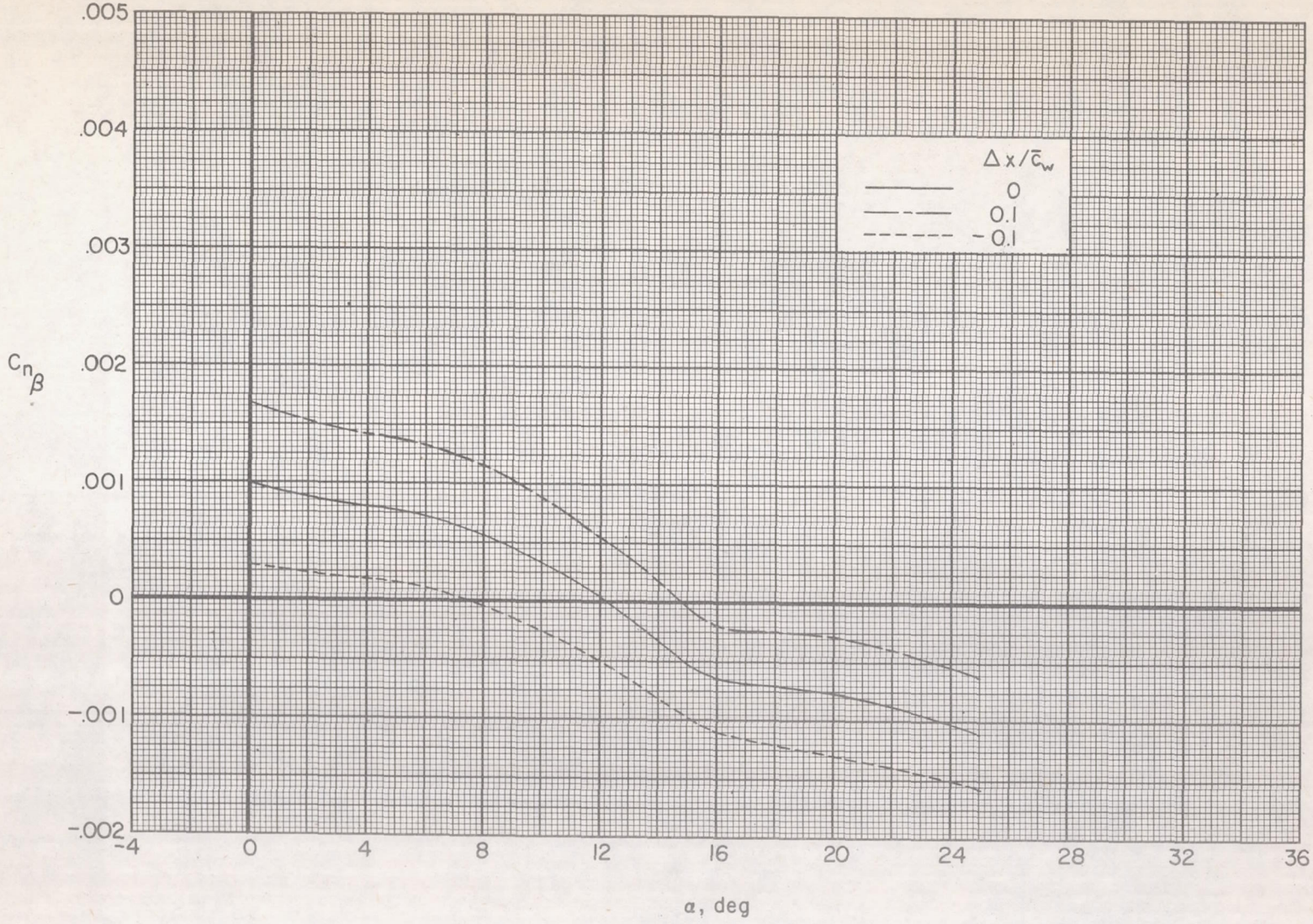


Figure 16.- Effect of center-of-gravity position on directional stability characteristics. Delta wing; $S_c/S_w = 0.096$; M = 2.01.

NACA - Langley Field, Va.